HAPTIC FEEDBACK DEVICE FOR INCREASED BCI LEARNING RATE

Moria Fisher, Craig Lenders,
and Courtney Normand

ME 450, Winter 2010
Team 19

Co-sponsor: Dr. Jane Huggins
Departments of Physical Medicine and Rehabilitation
and Biomedical Engineering
University of Michigan
Ann Arbor, MI 48109

Co-sponsor/Instructor: Dr. Brent Gillespie
Department of Mechanical Engineering
University of Michigan,
Ann Arbor, MI 48109

April 20th, 2010

ABSTRACT

Using a non-invasive electroencephalography (EEG) skullcap, electrical signals pertaining to mu rhythms (8-12 Hz) and beta rhythms (18-25 Hz) can be acquired from a subject either physically moving or imagining a movement. Brain-computer interfaces (BCIs) have been developed to acquire EEG signals and produce useful command signals. To be successful for use with BCI technology, the user must undergo a tedious and time intensive learning process in order to control EEG signals. Dr. Jane Huggins, the principal investigator of the University of Michigan Direct Brain Interface (UM-DBI) project found that it takes a user 20 to 25 sessions of an hour duration to control an on-screen cursor using BCI technology. Currently, the only BCI feedback available at the UM-DBI project is visual. We believe that the addition of a sensory feedback that imitates a natural muscle movement could improve the BCI learning process, making BCI technology available and appealing to a wider range of patients both locally and worldwide. In order to achieve this increased learning rate, we aim to create a device that not only mimics the motion imagined by the user, but also creates this motion in such a way that the user feels a sense of agency. The haptic feedback device designed by ME 450 Team 19 will be incorporated into the UM-DBI project BCI set up to test if the learning rate for BCI mastery is increased.

TABLE OF CONTENTS

I. EXECUTIVE SUMMARY

Brain-computer interface (BCI) technology provides a communication pathway by translating EEG signals provided by a human user into a command recognized by a machine. Over the past four decades, interest in non-invasive BCI technology has increased with its realized application towards rehabilitation. Electric signals produced by the brain are monitored using electroencephalography (EEG), digitized, and processed using BCI software such as BCI2000 (http://www.bci2000.org/). The signal then produces a device-specific command which sends feedback to the user. Topics of debate pertaining to BCI technology include the best way to provide feedback to BCI users in order to increase the learning rate. It is generally accepted that a subject receiving feedback using a BCI has an increased performance compared to a subject not receiving feedback [7]. Currently the most common feedback options are visual and auditory and include lights, tones, moving bars, and cursors. Even though BCI training inherently uses feedback, only two previous studies (McFarland et al. [5] and Neuper et al. [6]) investigated the effect of feedback on the BCI learning process. Cincotti et al. [1] is the only study to have investigated the use of tactile feedback for an EEG based BCI.

This project is sponsored by Dr. Jane Huggins, a research associate professor affiliated with the University of Michigan Physical Medicine and Rehabilitation and the University of Michigan Department of Biomedical Engineering, and Dr. Brent Gillespie, an associate professor affiliated with the University of Michigan Department of Mechanical Engineering. Presently, the BCI technology used by Dr. Jane Huggins and the University of Michigan Direct Brain Interface (UM-DBI) project only provides visual feedback. On average, Dr. Huggins has found it takes a user 20 to 25 sessions of an hour duration to learn BCI technology; however, the average person with ALS, when surveyed, was only willing to spend 2 to 5 sessions. Dr. Huggins and Dr. Gillespie propose that by introducing haptic feedback it may be possible to accelerate the learning process, allowing BCI technology to be a more attractive rehabilitation resource for a person with ALS. The outcome of this project is to produce a device that will seamlessly provide haptic feedback to the user that imitates a natural muscle movement. Dr. Huggins can then use the device to research the effect of haptic feedback on the BCI learning process.

In order for the haptic feedback introduced by this project to improve the BCI learning process it must be able to simulate a muscle movement without adding further disruptions to the learning environment. The most important project requirements are that the device 1.) provides corresponding feedback, 2.) is simple, 3.) is audibly absent, 4.) is adjustable for user-specific hand size, and 5.) has varying feedback levels. These project requirements translate to the respective engineering specifications of less than 0.125 second response time, less than two moving components, a noise level less than five decibels, three size settings, and three feedback levels, including the default “off” setting. Additionally, the motion caused by the device should create a sense of agency for the user. This allows the user to believe that his or her body generated the motion which was actually produced by the device.

The project plan includes design planning stages, prototyping phases, redesign periods, and a week of subject testing with the UM-DBI project prior to the Design Expo. Additional provisions will be made to comply with the $400 budget provided by our sponsors.

II. PROJECT DESCRIPTION

This project is sponsored by Dr. Jane Huggins, a research assistant professor affiliated with the University of Michigan Physical Medicine and Rehabilitation and the University of Michigan Department of Biomedical Engineering, and Dr. Brent Gillespie, an assistant professor affiliated with the University of Michigan Department of Mechanical Engineering.

In Dr. Huggins' lab, the current brain-computer interface (BCI) used only provides visual feedback. Presently it takes approximately 20 hour-long sessions for patients to achieve 80% target accuracy, however Dr. Huggins found by surveying patients with ALS that they were only willing to participate in two to five sessions of an hour duration to learn BCI technology. Dr. Huggins is interested in using haptic feedback in order to increase the BCI learning rate and allow BCIs to be more attractive to patients. The outcome of this project is to produce a device that will provide haptic feedback to the user that imitates a natural muscle movement. Dr. Huggins can then use the device to research the effect of haptic feedback on the BCI learning process. We hypothesize that in order to effectively reduce the learning rate that the subject has a sense of agency over the motion created by the haptic device. This means the subject must believe that the resulting sensory stimuli generated from the device is due to the subject's own actions. Thus, for the project to be accepted as a viable learning tool, the action created by the device must be believable.

The sensory stimuli that individuals experience on a daily basis can be classified as afferent or efferent, where afference corresponds to the brain's direct reception of signals from the body and efference corresponds to the signals sent by the brain to the periphery [9]. In 1950, the modern concept of "efference copy" was introduced by Erich von Holtz and H. Mittelstadt [10]. They found that each time an individual sends an efferent signal from the cognitive area of the brain to the motor command center, copies of the efferent signal are sent to the perception area of the brain. In the perception area, the efferent copy travels through the internal model of the outside world that creates expectation. This expectation is then compared with the afferent response the individual feels following the motor command. The interpretation of these terms with respect to their location in the brain is illustrated in Fig. 1 below.

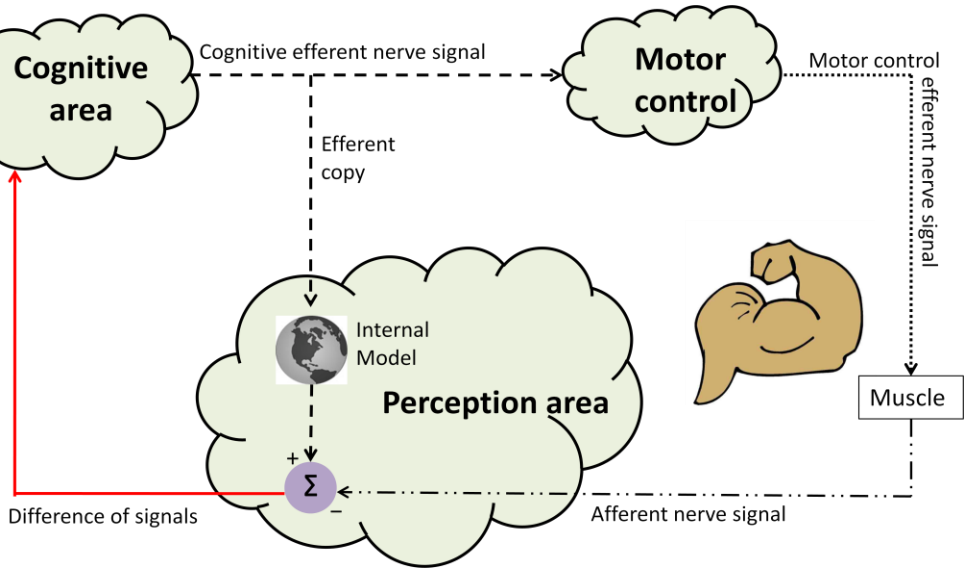

Figure 1: Location of brain signals

They further hypothesized that when the difference between the afferent and efferent signals is zero, the action is called re-afferent, meaning that the person's expectations match what actually occurs. However, if the difference is non-zero then the action is ex-afferent, and expectation does not match experience. In his subsequent study of the "re-afference principle", von Holst demonstrated that organisms are able to separate re-afferent stimulus from ex-afferent [9]. This ability to distinguish between re-afference and ex-afference is critical for human beings to understand their present surroundings. If the device used for haptic feedback is to be seamlessly integrated into the learning environment, it is important the action is re-afferent and not ex-afferent so that concentration can be maintained. The afferent types associated with incorporating an external device for the arm are illustrated in Fig. 2 below.

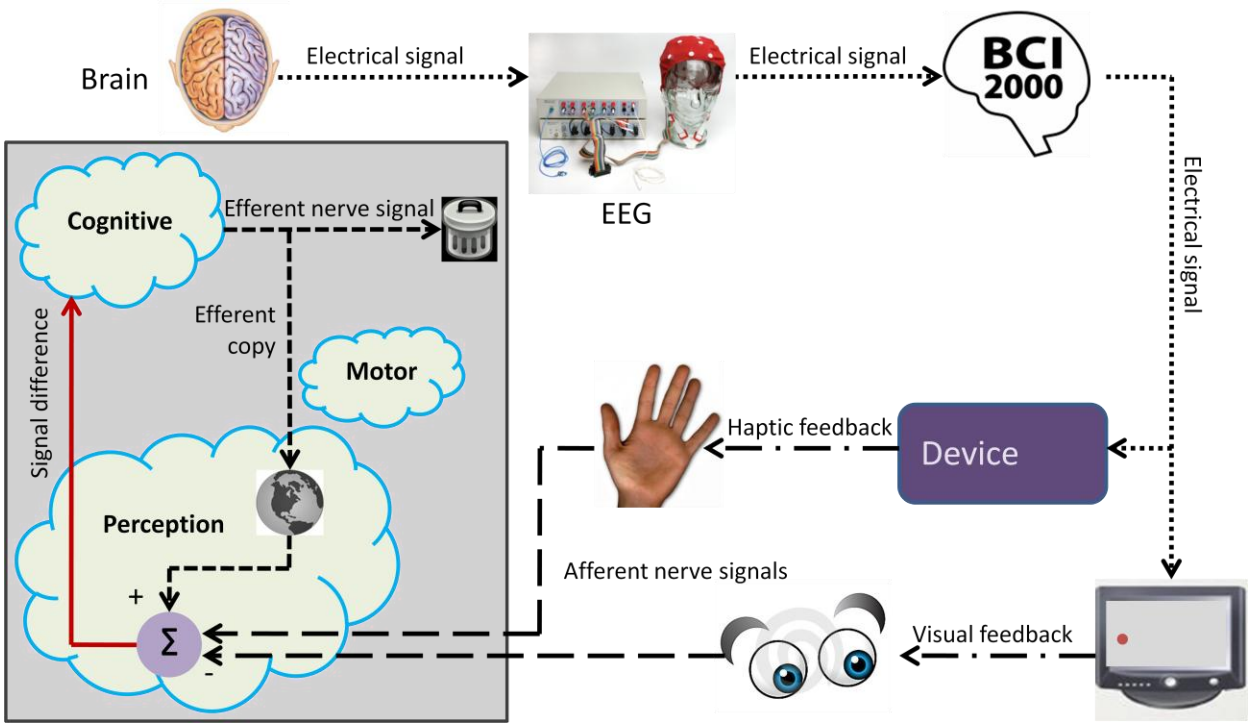

Figure 2: Project schematic

III. TECHNICAL BACKGROUND

In order to create a device that can be integrated into the BCI process, it is necessary to look at the history of BCI technology and the current research surrounding the use of feedback in BCI learning.

III.1. Background Information

The origins of EEG signals can be traced back to 1929, when Hans Berger demonstrated it was possible to record EEG signals from intact skulls of human subjects. In 1973, Jacques Vidal, who was researching at the Brain Research Institute at UCLA, published research regarding brain-computer communication [11]. Non-invasive BCIs, which use signals from an EEG skullcap instead of invasive surgery, were introduced as a means to use EEG to provide computer commands. McFarland et al. [8] conducted a study (33 adults, 90 trials each) examining relationships of mu rhythms (8-12 Hz) and beta rhythms (18-25 Hz) generated from actual and imagined movement. They found movement and imagery specific to

right and left sides were similar in frequency and topography but differed in magnitude. They also found that even if low level muscle movement occurred when subjects were imagining a movement the effects of imagery were not changed. The similarities discovered between generated signals for both imagined and actual movements showed the strong influence imagery has on EEG communication. By demonstrating that EEG signals are similar whether the movement is simply imagined or physically occurs, non-invasive BCI technology can expand to cases of muscle rehabilitation beyond ALS or brain stem strokes.

III.2. Current Research

Even though BCI feedback is necessary for mastering a BCI system, only two previous studies (McFarland et al. [5] and Neuper et al. [6]) investigated the effect of visual and auditory feedback on the BCI learning process. To date, Cincotti et al. [1] is the only study to have investigated the use of tactile feedback for an EEG based BCI.

IV. PROJECT REQUIREMENTS AND ENGINEERING SPECIFICATIONS

During initial meetings with Dr. Jane Huggins and Dr. Gillespie, the project requirements were discussed and compared to the previous ME 450 BCI-haptic feedback project (Fall 2007). These requirements were then translated into engineering specifications and corresponding target values that were to be met in the device design, as seen in Table 1 below.

Table 1: Project requirements to engineering specifications

Project Requirements	Engineering Specifications	Target Values
Corresponding feedback	Response time	≤ 0.125 seconds
Audibly absent	Noise level	≤ 5 dB or constant
Initial adjustability for comfort	Size settings	≥ 3
Simple	Number of moving components	≤ 2
Varying feedback levels	Feedback settings	≥ 3
Size	Width × length	20” × 20”
Portable	Weight & set-up time	≤ 25 lbs & < 15 minutes

In addition to these requirements, safety of the user was also of the utmost concern. Safety was characterized by the engineering specifications of response time, size settings, and feedback settings. A maximum possible force will also be included in the device to add an additional safety feature. A full comparison of all project requirements and engineering specifications can be found in the form of a QFD in Appendix A.

IV.1. Corresponding Feedback

In order for the sensory feedback to aid in the BCI learning process, the device’s response must correspond with the BCI signal. As specified by Dr. Huggins, the goal is to design a device with a response time of less than 0.125 seconds. This time should result in parallel haptic and visual feedbacks, reinforcing the learning process.

IV.2. Audibly Absent

In order to perform a controlled experiment, the device must be audibly absent. The user of the device cannot know when engagement occurs, because any auditory cues will interfere with the haptic feedback learning process. In order to fulfill this requirement, the device will either operate under the

five dB level or the noise level will remain constant, with no discernable difference between engaged and disengaged. Five dB was chosen because a whisper is about 15 dB, and a level a little bit smaller would be reasonable to ensure that the device does not cause disruption to the BCI learning process.

IV.3. Initial Adjustability for Comfort

To avoid additional disturbances to the BCI process, the user must be comfortable throughout experimentation so clear results can be obtained. To ensure comfort, the device will have at least three initial size settings to choose from.

IV.4. Simple

Because the device will be used in experiments and the technicians do not have mechanical backgrounds, two or less moving components should be used in order to minimize maintenance requirements and set-up complexity.

IV.5. Varying Feedback Levels

The device must offer different levels of feedback depending on the intensity of the signal received from the BCI. In practice, this would translate to a greater haptic response to correspond to a stronger signal. The device will provide at least three levels of feedback, including a default "off" setting.

IV.6. Size

The device must be able to be incorporated into the Rehabilitation Engineering BCI testing facilities and maintain a comfortable position for the user's arm. The length and the width of the device both must be less than 20 inches.

IV.7. Portable

The device must be portable so that it can be moved from the lab to a patient's home or other labs. To ensure the average person can transport the device, it must not weigh more than 25 pounds. Additionally, the set-up time must be less than 15 minutes in order to allow for the timely completion of experiments.

V. CONCEPT GENERATION

Since the aim of the project is to create a device that is re-afferent for use with BCI, a functional decomposition was first performed to visualize the locations of feedback associated with BCI. A block diagram of the project with both visual and haptic feedback can be seen in Fig. 3, below.

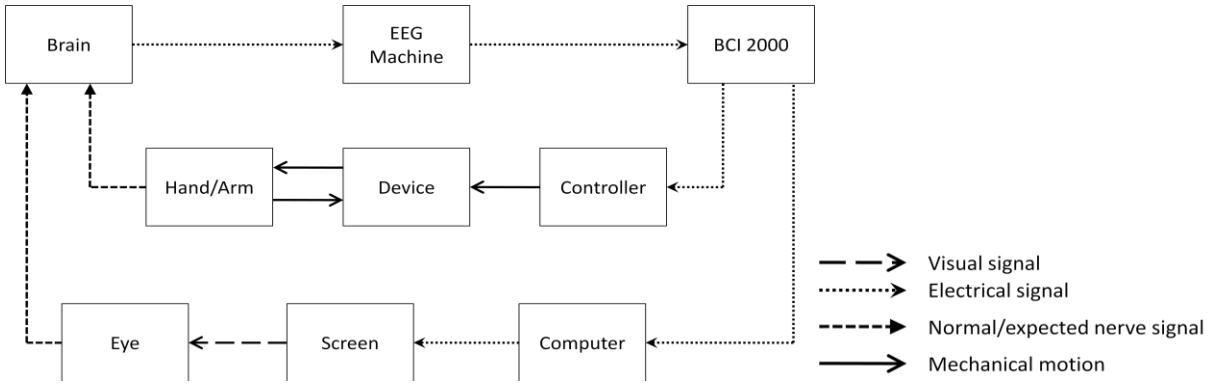

Figure 3: Functional decomposition

In order to initiate concepts that met the project requirements and engineer specifications, we first looked to typical haptic motions which could be based on both imagined and real motion. If the device incorporates the concept of re-afference then the motion must be natural for the user. Therefore we brainstormed everyday hand motions such as squeezing, moving, and rotating. We also investigated the idea of using an illusion of hand movement as a type of feedback. The generated concepts, organized by movement type, are shown in Fig. 4 below.

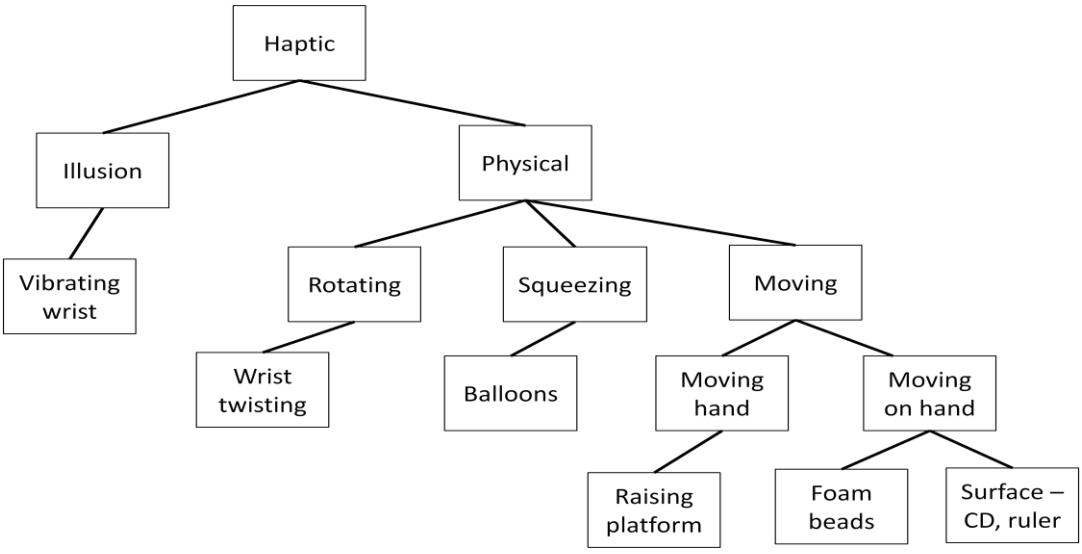

Figure 4: Idea taxonomy

V.1. Illusion-based Haptic Feedback

Research has been done in the field of wrist tendon vibration where vibrations are applied to specific tendons in the wrist to create an illusion of the hand extension and contraction. It was proposed that if the vibration was initiated by EEG activity then the user could experience an illusion that correlates with the initial imagery of a hand motion. This illusion would produce an afferent signal that comes from within the body, and therefore could be re-afferent, providing an initial attraction to this idea. Design 1, in Fig. 5 below, shows the proposed locations of wrist vibration to create strong illusions of movement.

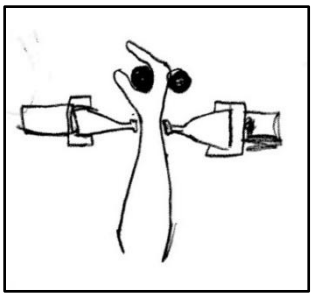

Figure 5: Design 1

After meeting with Dr. Bernard Martin, an associate professor at the University of Michigan who researches human sensorimotor control systems, we realized the challenges of wrist tendon vibration were too large to be effectively incorporated with BCI. Such challenges included varying response times of 1 to 30 seconds for an illusion to be generated, variability of vibration amongst users, and the need

for the user to be mobile following each illusion which could severely disrupt the BCI learning environment.

V.2. Movement-based Haptic Feedback

Movement based feedback includes any device that physically moves the hand directly or moves a material with respect to the hand. The four main categories which are based on common hand uses are explained in the subsequent sections.

V.2.1. Hand squeezing

Our initial ideas for hand squeezing were based on a previous haptic feedback device created in Dr. Gillespie's laboratory. While the imagery used to produce strong signals for use with BCI varies between users, squeezing the hand is commonly imagined since it involves a large range of motion as well as an imagined sense of the skin pulling to make a fist. Design 2, pictured in Fig. 6 below, features a balloon-like object that would expand and contract using water, simulating a fist opening and closing. Design 3, shown in Fig. 7 below, is similar except that the hand is placed inside object, where water pressure would be felt both inside and outside the fist. The intensity of signal would correlate to the degree of expansion of the fist for Design 2 or the degree of contraction of the fist in Design 3.

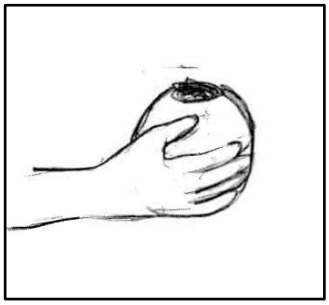

Figure 6: Design 2

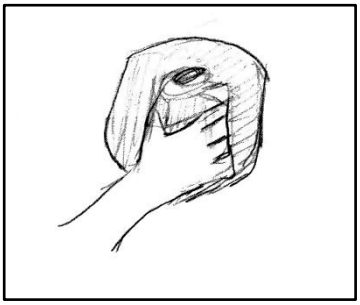

Figure 7: Design 3

V.2.2. Wrist rotation

The basic idea behind a rotating platform design is to cause the hand to move without changing the area of surface contact. By placing the hand on top of a platform that is capable of rotating back and forth, as shown in Fig. 8 below, the only change is the intensity of the movement and not the location of forces.

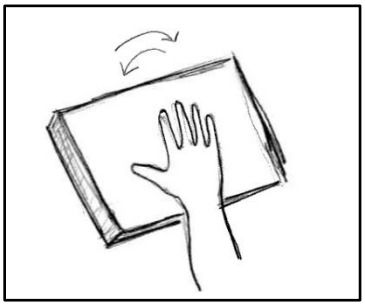

Figure 8: Design 4

V.2.3. Finger raising

The idea behind having a platform move the user's fingers axially is similar to the rotating platform shown above in that the fingers have constant contact with the moving object. From previous discussion with Dr. Huggins and her assistant, Carmela, it was discovered that finger movement is also a

typical imagined movement. Since imagination of moving fingers has been proven to create strong EEG signals, it is believed that finger raising, shown in Fig. 9 below, is thereby a logical haptic response.

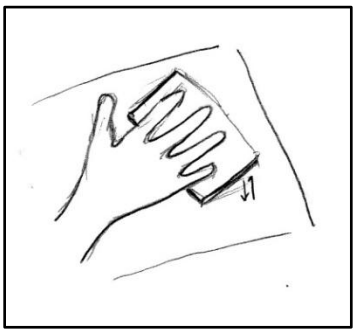

Figure 9: Design 5

V.2.4. Moving surface

In continuing with the integration of re-afference, brainstorming also included designs which moved materials under or around the hand. We initially were drawn to using a fan, as shown in Fig. 10 below, to blow air on the hand in an enclosure since pressure due to winds is a common recognizable feeling. The intensity of the fan would correlate to the intensity of the EEG signals and could move material (air) quickly over the hand. Design 7, shown in Fig. 11 below, is similar in that a material would move underneath the hand, such as a disc constantly spinning, but would also include varying textures to correspond with the EEG signals.

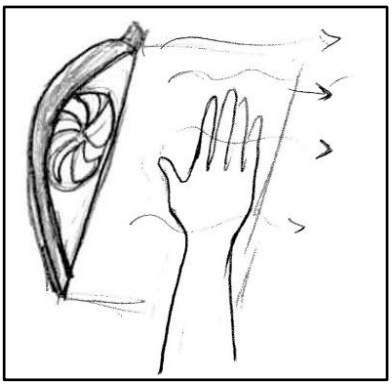

Figure 10: Design 6

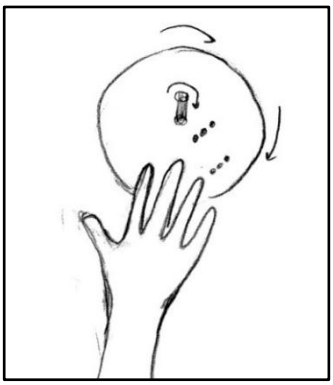

Figure 11: Design 7

V.3. Concept Evaluation and Selection

The seven generated designs were evaluated on their feasibility and their ability to create a natural motion. The following three designs were determined to be the most viable options in moving forward in the selection process:

- Design 4: Wrist rotation
- Design 5: Finger raising
- Design 7: Moving material

These three designs were selected because they each would create a natural motion or feeling that the user would feel. Design 4 would simulate the user twisting their wrist. Design 5 would simulate someone lifting their fingers while their palm stays level. Design 7 would simulate rubbing your fingertips across a surface. More details on each of these designs are shown in the following sections.

V.3.1. Evaluation of engineering specifications

First, each of the three designs was evaluated based on whether or not they met the five most important engineering specifications as determined by the QFD (see Appendix A). This comparison can be found in Table 2 below, where a score of "1" denotes compliance with the engineering specification and a score of "0" denotes failure to comply. The total score based on engineering specifications was determined by first multiplying the weighted value of each specification (based on the QFD analysis in Appendix A) by the score and adding each of these products for the specific designs.

Table 2: Engineering specification comparison for three final designs

	Number of Moving Components (≤2)	Noise Level (≤5dB or constant)	Response Time (≤0.125 s)	Size Settings (3)	Feedback Settings (2)	
Weighted Value	6	6	10	6	6	**Total Score**
Wrist Rotation	1	1	1	1	1	34
Finger Raising	1	1	1	1	1	34
Moving Material	1	1	1	1	1	34

As visible in Table 2, all of the chosen designs comply with the engineering specifications, so the total score for each design is the same. Therefore, these criteria alone are not enough to select the optimal design.

V.3.2. Evaluation of re-afference

The objective of the device is to make the user believe that they caused the motion that the device actually causes. We are trying to create a device that provides the most believable motion to the user. In order to evaluate the level of believability for the three selected designs, we used the principle of re-afference and signal differences as seen previously in Fig. 1, p. 5. By canceling signals generated from the device with those created from expectation in the internal model, a motion can become re-afferent and provide the user a sense of agency. The breakdowns of these signals for each of the three designs are shown in the subsequent sections.

V.3.2.1. Wrist rotation

The expected signals and the signals generated by the device are listed in Table 3 below.

Table 3: Wrist rotation signal comparison

Expected signals	Device generated signals
Muscle contraction	Muscle contraction
Skin stretch	Skin stretch
Relative motion to air	Relative motion to device
Energy expenditure	Pressure felt

A schematic comparison of the signals generated from expectation (i.e. the internal model) and the signals generated from device can be seen in Fig. 12, p.14. The signals that are not common to both

expectation and actual experience are denoted by dotted lines. The difference in signals is then sent to the cognitive area of the brain to be analyzed.

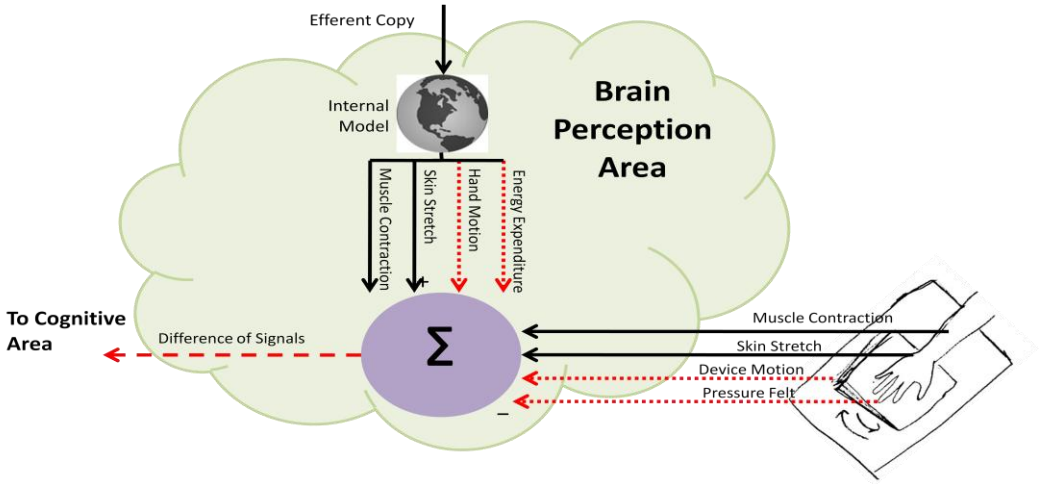

Figure 12: Wrist rotation brain mapping

V.3.2.2. Finger raising

The expected signals and the signals generated by the device are listed in Table 4 below.

Table 4: Finger raising signal comparison

Expected signals	Device generated signals
Muscle contraction	Muscle contraction
Skin stretch	Skin stretch
Relative motion to air	Relative motion to device
Energy expenditure	Pressure felt

A schematic comparison of the signals generated from expectation (i.e. the internal model) and the signals generated from device can be seen in Fig. 13 below. The signals that are not common to both expectation and actual experience are denoted by dotted lines. The difference in signals is then sent to the cognitive area of the brain to be analyzed.

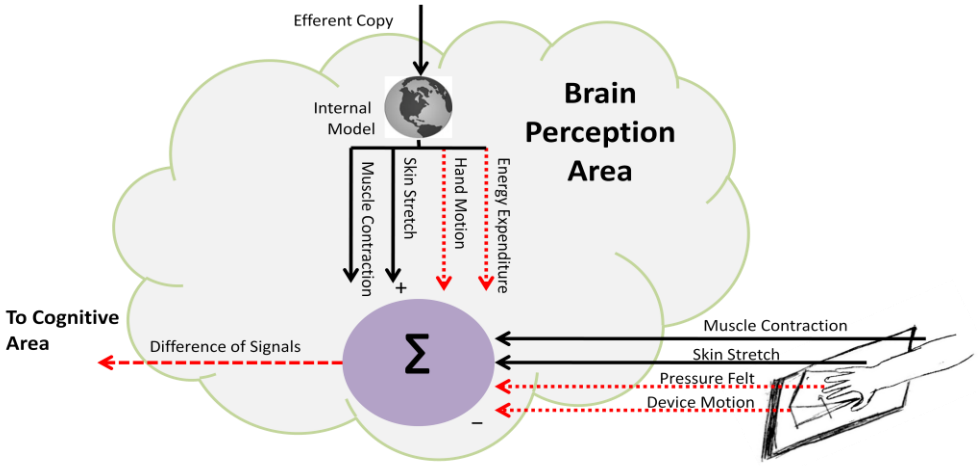

Figure 13: Finger raising brain mapping

V.3.2.3. Moving surface

The expected signals and the signals generated by the device are listed in Table 5 below.

Table 5: Moving surface signal comparison

Expected signals	Device generated signals
Tactile feeling Energy expenditure Muscle movement	Tactile feeling

A schematic comparison of the signals generated from expectation (i.e. the internal model) and the signals generated from device can be seen in Fig. 14 below. The signals that are not common to both expectation and actual experience are denoted by dotted lines. The difference in signals is then sent to the cognitive area of the brain to be analyzed.

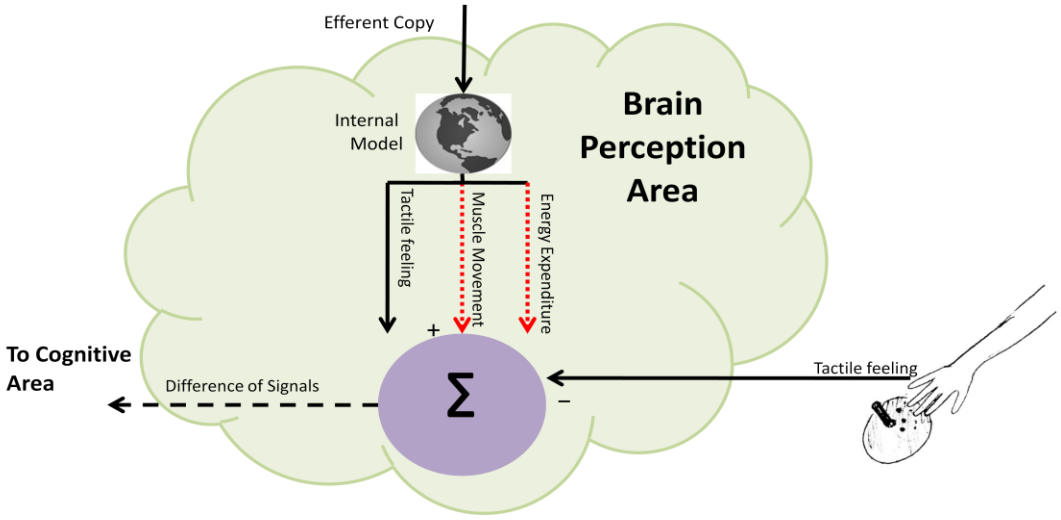

Figure 14: Moving surface brain mapping

V.4. Final Design Selection

In order to determine the final design, we built basic prototypes of the three chosen concepts to gage the believability of each design. These prototypes were used to perform an experiment to find which design will create the most natural and believable motion. The methods, results, and analysis of this study are shown in the subsequent sections.

V.4.1. Experimental methods

The experimental methods consist of the apparatuses used for testing, subjects, and the protocol followed by the test administers.

V.4.1.1. Experimental apparatuses

Three designs were created for each of the selected concepts in order to test and compare the believability of each concept. Design A consisted of two platforms covered with 2” foam pads resting under both hands. The platform resting under the right hand was on an incline to allow the administrator access. The setup for Design A can be seen in Fig. 15, p.16.

Figure 15: Design A setup

Design B consisted of two smooth sheets of paper, with the left piece of paper was attached by adhesive to the testing surface. The setup for Design B can be seen in Fig. 16 below.

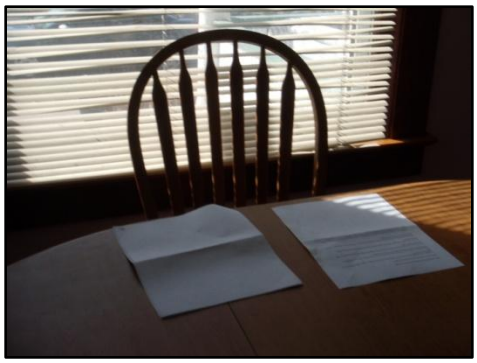

Figure 16: Design B setup

Design C consisted of a large metal cylinder and a soccer ball each with 2" foam pads attached, allowing both wrists to rest at approximately the same height. The metal cylinder was hollow in order for the administrator to be able to rotate the subject's hand. The setup for Design C can be seen in Fig. 17 below.

Figure 17: Design C setup

V.4.1.2. Experimental subjects

A total of twenty subjects (13 females, 7 males) were tested. Subjects tested ranged from 20 to 23 years of age. Subjects were selected on a volunteer basis with no incentive for completion of the experiment.

V.4.1.3. Experimental protocol

The order of Design A, B, and C was randomized for each subject to eliminate any biased based on the order the designs were tested. All three group members administered the tests to the subjects. A timer was started once the administrator began moving the device to simulate the subject's motion. Subjects were asked to stop once they had reached a state of believability.

During Design A, the subject was initially asked to raise both hands slowly away from the foam and back down. The subject was then asked to continue raising only the left hand. The administrator then raised the platform under the subject's right hand to match the motion of the left. The subject was asked to continue hand raising for 1-2 minutes.

During Design B, the subject was initially asked to slide both hands along the paper in opposite directions. The subject was then asked to continue only sliding the left hand along the paper. The administrator then moved the paper underneath the right hand, simulating the sliding motion of the fingers. The subject was asked to continue moving his hand over the paper for 1-2 minutes.

During Design C, the subject was asked to place his left hand on the foam pad of the soccer ball and his right hand on the foam pad of the cylinder. The subject was initially asked to rotate both hands in opposite directions. The subject was then asked to continue rotating only the left hand. The administrator then rotated the metal cylinder in the opposite direction as the left hand. The subject was asked to continue rotating his left hand for 1-2 minutes.

Following each test, subjects were asked questions pertaining to the design and to report how long (if applicable) it took to feel like the motion was caused by the subject and not the test provider. After all three designs were presented, the subject was asked to choose the motion which felt the most natural.

V.4.2. Experimental results

Experimental testing was completed on twenty subjects over a 10 day time period. The results of the experiments can be found in Fig. 18 below. Fourteen subjects reported design A was the most believable motion. Five subjects reported that Design B was the most believable motion. No subjects reported Design C to be the most believable motion. One subject was undecided between Design A and Design B regarding which was the most natural movement. No other correlations were found between the final design selection, the order of provided tests, and the gender or age of the subject. Additional results can be found in Appendix B.

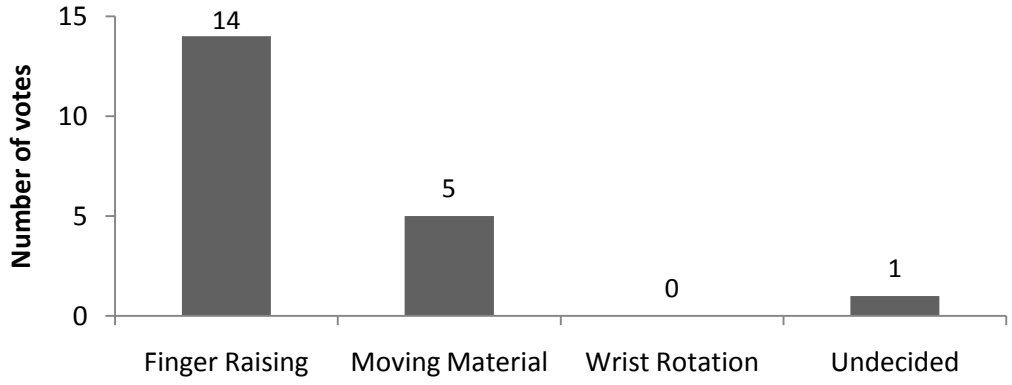

Figure 18: Results of subject testing votes for design concept

V.4.3. Experimental analysis

Based on the results generated from experimental testing on concept prototypes, we believe Design A or "Finger raising" is the best design. Finger raising meets the engineering specifications and won in the subjective testing of which is the most believable motion. During experimentation it was noticed that finger raising introduced a level of discomfort when the subject's fingers were hyperextending, therefore, we have altered the design to raise the fingers from rest to extension instead of raising from extension to hyperextension, as detailed in the following section.

VI. CONCEPT DESCRIPTION

Once the decision to proceed with the finger raising method was chosen, a preliminary concept was developed. Figure 19 shows the proposed concept in the resting position, where the fingers will be resting comfortably on the blue plate and the palm and forearm will be resting comfortably on the top of the frame. Figure 20 shows the extended position, where the fingers will be raised to an angle of 40°.

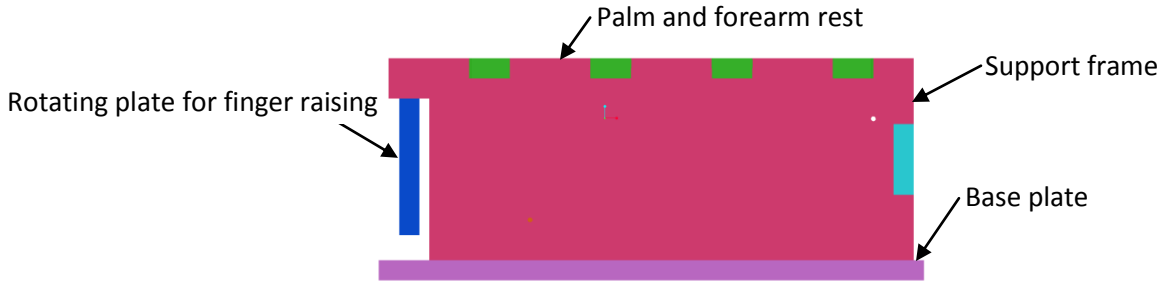

Figure 19: Proposed concept design in resting position

Figure 20: Proposed concept design in extended position at an angle of 40°

VI.1. Mechanical System Selection

The following two mechanical systems were explored in order to cause the plate to rotate, lifting the user's fingers: a pneumatic cylinder and a capstan drive motor.

VI.1.1. Pneumatic cylinder

One option for rotating the plate is to use a pneumatic cylinder. A pneumatic actuator works by converting potential energy of a compressed gas into kinetic energy, resulting in the displacement of an object. The compressed gas is allowed to expand by opening a valve. This gas then goes on to move a piston to move in the desired direction. This piston is in the form of a cylinder, and in our device, it would push the plate outward which would result in it rotating up due to a hinge attachment. Once moved to the desired place, the valve would close and a spring will return the piston to its original position. For our device, a microprocessor would control the valve which would therefore provide

control of the position of the rotating plate and illustrated by the flowchart in Fig. 21 below. A more detailed schematic of how this would work is shown in Fig. 22.

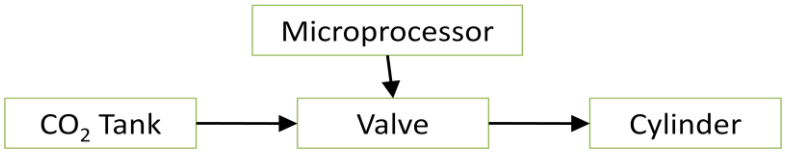

Figure 21: Flow chart for pneumatic cylinder system

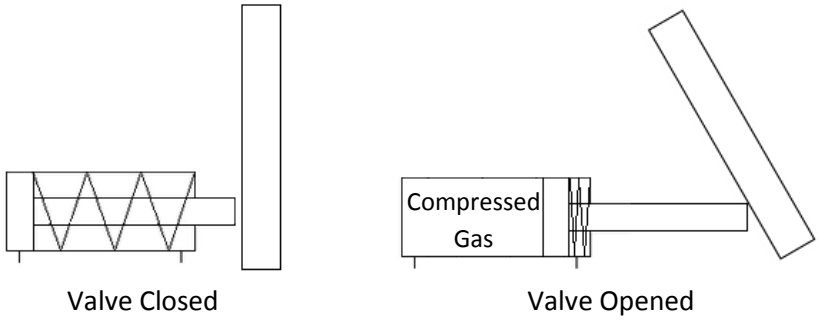

Figure 22: Schematic of pneumatic cylinder

VI.1.2. Capstan drive motor

The second available option discussed for rotating the plate is the use of a capstan drive motor. A capstan drive motor works by wrapping a cable around the shaft of a motor that is attached to a circular wedge shaped object at two points. As the motor shaft spins, it either wraps more cable or unravels cable, causing the wedge to move. This can be used in our device to attach the wire to two points on the outer radius of a wedge. As the motor shaft spins, the cable at one of the points will be pulled towards the motor, causing the wedge to rotate. The plate where the user's fingers will be is then attached to this wedge and rotates with it. Since it is a circular arc, it will act as a gear that meshes with the motor shaft acting as a second gear. A schematic of this system is shown in Fig. 23.

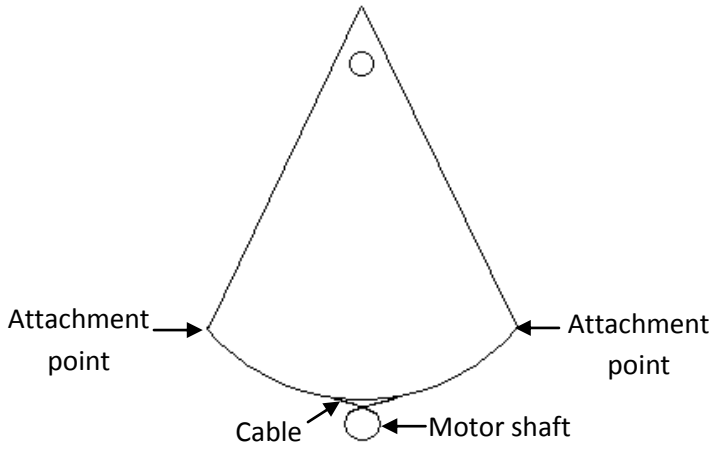

Figure 23: Schematic of capstan drive motor

VI.1.3. Evaluation of mechanical systems

After exploring both of these mechanical systems, we evaluated the available resources and how appropriate they would be for the device. In order to use the pneumatic cylinder, we would need to get a tank of pressurized gas, a controllable valve, and a pneumatic cylinder. None of these would be provided to us, and each would have to be purchased. A tank of pressurized gas is on average $50 and requires additional space in the lab. Furthermore, when it runs out, a new tank would need to be ordered and installed, requiring additional maintenance. Also, working with pressurized gas and a valve could be noisy, which creates another drawback to this option.

A capstan drive motor would need a wedge shaped object, a dc motor, and cable to wind around the motor shaft and wedge. A wedge can be easily fabricated in the machine shop, a dc motor can be provided by Professor Gillespie, and cable can either be provided by Professor Gillespie or will fit within our available budget. The capstan drive is quiet and is relatively simple to manufacture.

Due to the drawbacks to the pneumatic cylinder and the feasibility of the capstan drive motor, we will proceed with our design by using a capstan drive motor for the mechanical system required to rotate the plate where the user's fingers will be positioned.

VII. FINAL DESIGN

The following sections detail the final design for the device. They will describe a number of parameters used while creating the design.

VII.1. Final Design Overview

The final design for the haptic feedback device includes a capstan drive motor system that drives a rotating plate that will cause the fingers to lift. The design in the finger resting position can be seen in Fig. 24, p.21. The components labeled in the figure can be found in Table 6, p.21, which lists all system components, the quantity and the material.

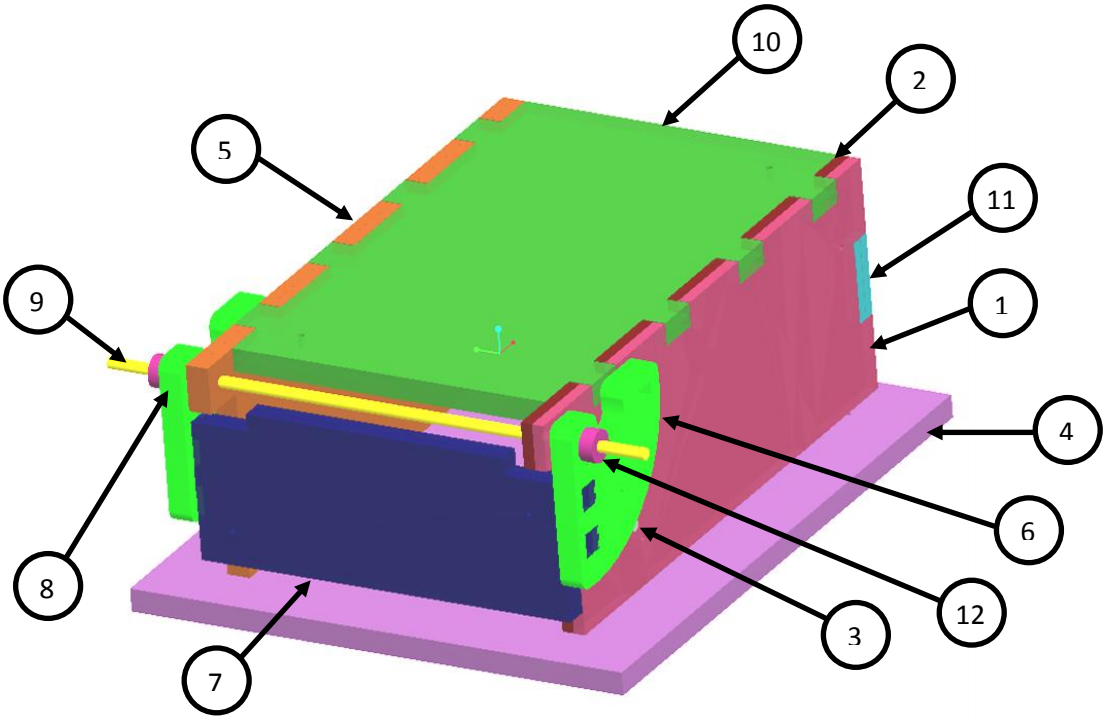

Figure 24: Final design in isometric view

Table 6: Component as seen in Fig. 24 above

Number	Name	Quantity	Material
1	Motor side 1	1	Baltic birch
2	Motor side 2	1	Baltic birch
3	Drive motor	1	Maxon RE40, Model No. 178867
4	Motor stand base	2	Baltic birch
5	Frame side	2	Baltic birch
6	Capstan drive wedge	4	Baltic birch
7	Rotating plate	2	Baltic birch
8	Bearing	2	McMaster-Carr, Part No. 426T15
9	Shaft	1	McMaster-Carr, Part No. 1257K66
10	Frame top	1	Baltic birch
11	Back	2	Baltic birch
12	Shaft collar	2	McMaster-Carr Part No. 6436K32

Figures 25 and 26 show the device from the side in both the resting and the extended positions. Full assembly drawings along with a complete BOM can be found in Appendix C.

Figure 25: Side view in resting position

Figure 26: Side view in extended position

VII.2. Determination of Materials

Once the final design was determined, the materials to be used were then chosen based on reasons outlined in the following sections.

VII.2.1. Main components

The frame, base, and the wedges are to be made out of Baltic birch. This material was chosen in order to comply with the requirement that the design be lightweight and easily maintained. Additionally, the material was readily available in Dr. Gillespie's Haptix Laboratory

VII.2.2. Covering

In order to ensure comfort and hygiene for the device, neoprene was chosen to cover the frame top and rotating plate. Neoprene, also known as polychlorophene, is the primary material in wetsuits, and is popular because of its high chemical stability and resistance to oils and water. Neoprene usually costs around $2.50/lb. The CES EduPack properties for neoprene can be found in Appendix C.

VII.3. Determination of System Requirements

In order to determine the parameters of all parts used in a capstan drive system it was necessary to break down the requirements of the system and translate them to motor specifications. These requirements include the torque generated by the weight of the hand and the plate at the rotating plate's point of rotation, the torque generated by the motor, and the mechanical advantage required to safely operate the system. For the purpose of the project, we were provided with a RE 40 Maxon Motor No. 178867.

VII.3.1. Determination of torque at joint

We first created a free body diagram, shown in Fig. 27 below, for the system to include the forces due to the weight of the fingers and the forces due to the weight of the plate underneath the hand.

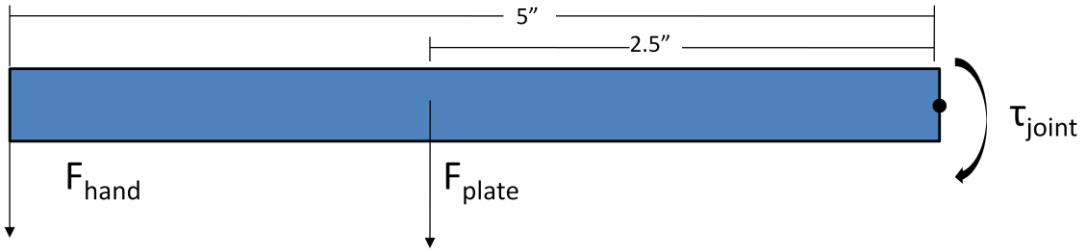

Figure 27: Free body diagram of rotating plate

The force required to lift the hand, designated as F_{hand} in Fig. 22 above, was measured during maximum extension (θ=90°) using a Zebco Deliar 228 Spring gauge to be 0.75 lbs approximately 5” away from the point of rotation. This distance was determined to be 5” based on the average finger length for a human. The torque generated due to the force of the hand, τ_{hand}, is calculated in Eq. 1 below, where r_{hand} is the distance from the location of the hand force to the joint of rotation.

$$\tau_{hand} = r_{hand} \cdot F_{hand} = 5 \text{ in} \cdot 0.75 \text{ lb} = 3.75 \text{ lb-in} \quad \text{(Eq. 1)}$$

The force due to the plate, designated as F_{plate} was measured based on the volume of the plate, V_{plate}, and the density of Baltic birch, ρ_{birch}. The calculations of the torque due to the plate, τ_{plate}, can be found using Eq. 2, p. 23, where r_{plate} is the distance from the location of the plate force to the joint of rotation.

$$\tau_{plate} = r_{plate} \cdot F_{plate} = r \cdot \rho_{birch} \cdot V_{plate} = 2.5 \text{ in} \cdot 0.026 \text{ lb/in}^3 \cdot 20 \text{ in}^3 = 1.3 \text{ lb-in} \qquad \text{(Eq. 2)}$$

The total torque felt by the joint of rotation, τ_{joint}, is calculated by adding the torque due to the plate and the torque due to the hand, as seen in Eq. 3, below. This torque is equal to the torque of the wedge used in the capstan drive, τ_{wedge}, since the wedge and plate move concurrently.

$$\tau_{joint} = \tau_{wedge} = \tau_{hand} \cdot \tau_{plate} = 3.75 \text{ lb-in} + 1.3 \text{ lb-in} = 5.05 \text{ lb-in} \qquad \text{(Eq. 3)}$$

In order to ensure safety within the design, a safety factor of two was added. This means that the torque felt by the wedge is reported to be twice that calculated or 10.10 lb-in.

VII.3.2. Cable selection

With the direction of Professor Gillespie we looked at uncoated stainless steel cable manufactured by Sava cable. It was determined that a cable with a minimum breaking strength of 40 lbs would be appropriate for the system. A 7 x 7 construction, seven strands with seven wires in each strand, was chosen to ensure durability and longevity. The nominal cable diameter of Sava cable No. 2018 was found to be 0.018 inches at a cost of $0.447/ft. The cable arrangement is illustrated in Fig. 28 below.

Figure 28: 7 x 7 arrangement

VII.3.3. Determination of wedge radius

The radius of the wedge used in the capstan drive is determined using the torque needed at the joint, the diameter of the cable, and length the wedge must travel to rotate the plate. Before determining the radius of the wedge used in the system, the maximum and minimum wedge radii were found to ensure a factor of safety in wedge design.

VII.3.3.1. Determination of minimum wedge radius and associated cable parameters

We calculated the radius of the wedge using the lowest mechanical advantage to determine the smallest possible wedge before torque is lost in the system, i.e. no guaranteed direct drive. Based on the specification sheet provided by Maxon Precision Motors, Inc., we were able to locate the recommended range for the motor, shown in red in Fig. 29, p. 24. As seen in Fig. 29, Maxon reports motor parameters in SI units. However, we will be converting these values into Imperial units throughout the following discussion.

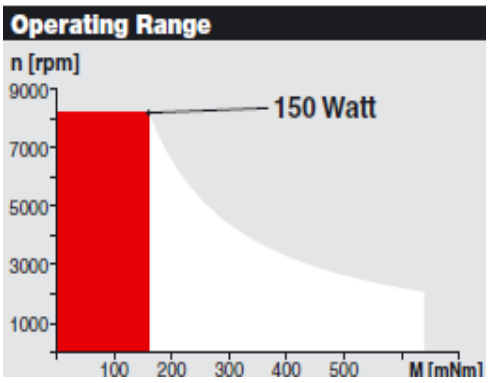

Figure 29: Operating range of RE 40 motor [12]

Based on the continuous operating range, the maximum allowable torque would be 150 Nmm, or 1.32 lb-in. Using the ratio of wedge torque to shaft torque as a gearing ratio, the minimum wedge radius, $r_{wedge,min}$, can be determined based on the radius of the motor shaft, r_{shaft}, which is 0.24 in, as shown in Eq. 4.

$$r_{\text{wedge,min}} = \frac{\tau_{\text{wedge}}}{\tau_{\text{shaft}}} * r_{\text{shaft}} = \frac{10.10 \text{ lb}-\text{in}}{1.32 \text{ lb}-\text{in}} * 0.24 \text{ in} = 1.81 \text{ in} \quad \text{(Eq. 4)}$$

The arc length of the wedge, d_{wedge} , can be then calculated using Eq. 5 below for angle of 40°, the angle through which the plate will move. This translates to the travel distance of the cable.

$$d_{\text{wedge}} = r * \theta * \frac{\pi}{180} = 1.26 \text{ in} \quad \text{(Eq. 5)}$$

The number of winds of the cable on the shaft, N, is then determined by divided the distance through which the wedge must move by the circumference of the shaft, as seen in Eq. 6 below.

$$N = 2 * \frac{d_{wedge}}{r_{shaft} * 2 * \pi} = 1.67 \text{ winds} \quad \text{(Eq. 6)}$$

It is then possible to determine the length of the cable winds, t_{cable}, on the shaft based on the cable's diameter, D_{cable}, and the number of winds using Eq. 7. A safety factor of 1.1 has been added to allow for "walking space" as the cable moves up and down the shaft.

$$t_{\text{cable}} = 2 * 1.1 * N * D_{\text{cable}} = 0.07 \text{ in} \quad \text{(Eq. 7)}$$

Since the maximum allowable motor shaft length is 0.42 inches, the thickness of cable required to move the wedge, 0.07 inches, falls below the maximum as shown in Table 7.

Table 7: Minimum wedge radius cable winding parameters

Wedge radius (in)	Arc length (in)	Required winds	Cable wind length (in)
1.81	1.26	1.67	0.07

VII.3.3.2. Determination of maximum wedge radius and associated cable parameters

The maximum allowable wedge radius was then determined by using the maximum length of the cable winds on the shaft before the cable would run out of "walking" room, calculating the maximum allowable winds to move through an arc length of 40°, and translating the number into the wedge's radius. These calculations were performed using Eqs. 4-7. As seen in Table 8 below, the maximum possible wedge radius under normal motor conditions would be 10 inches.

Table 8: Maximum wedge radius and cable winding parameters

Cable wind length (in)	Required winds	Arc length (in)	Wedge radius (in)
0.42	10.61	7.86	10.01

VII.3.3.3. Determination of wedge radius for system

Based on the geometrical constraints of the system, the allowable motor shaft length, and the cable radius, we determined an appropriate wedge radius to be 3.045 inches. This value falls within the calculated range of maximum and minimum wedge radii, therefore it is understood the wedge can generate enough torque to rotate the plate.

VII.3.4. Determination of mechanical advantage

The mechanical advantage, *M.A.,* of the system, equivalent to the capstan gearing ratio for the purpose of our system, is a constant calculated based on known input and outputs of the system in order to determine unknown design parameters. The mechanical advantage for the wedge in the capstan drive, calculated using Eq. 8 below, is based on the calculated radius of the wedge and the known radius of the shaft.

$$M.A. = \frac{r_{\text{wedge}}}{r_{\text{shaft}}} = \frac{3.045 \text{ in}}{0.24 \text{ in}} = 12.7 \qquad \text{(Eq. 8)}$$

VII.3.5. Determination of the shaft torque

Since the ratio of wedge radius to shaft radius is equivalent to the ratio of the wedge torque to the shaft torque, the mechanical advantage determined in Eq. 8 above was used to determine the variable operating torque required for the motor, τ_{motor}, as seen in Eq. 9 below.

$$\tau_{motor} = \tau_{wedge} * \frac{1}{M.A.} = \frac{10.10 \text{ lb}-\text{in}}{12.7} = 0.80 \text{ lb-in} \qquad \text{(Eq. 9)}$$

For the purpose of the project, we were provided with a RE 40Maxon Motor No. 178867. The calculated motor shaft operating torque of 0.80 lb-in translates to a torque of 90.4 Nmm, which falls within the recommended operating area shown in Fig. 29, p.24. Therefore, the motor is more than capable of providing the torque necessary to power our device.

VIII. BUILD PLAN

The following sections detail the fabrication of all components, the assembly process and the electrical connection details necessary for duplication of the device.

VIII.1. Main Component Fabrication

All wood parts were first laser cut to the dimensions shown in the engineering drawings in Appendix C. The wood used was ¼" thick, and to make the device sturdier, each piece was made of two identical pieces glued together to make ½" thick parts. The laser cutter in the Mechanical Engineering Machine Shop was used with the power set to 40%, speed set to 2%, and DPI set to 250. For each part, two dowel holes were cut into the pieces to align each pair correctly. Dowel pins were placed inside and the parts were placed on top of each other. Once aligned correctly, the parts were glued together with wood glue, clamped, and left overnight to dry, as seen in Fig. 30.

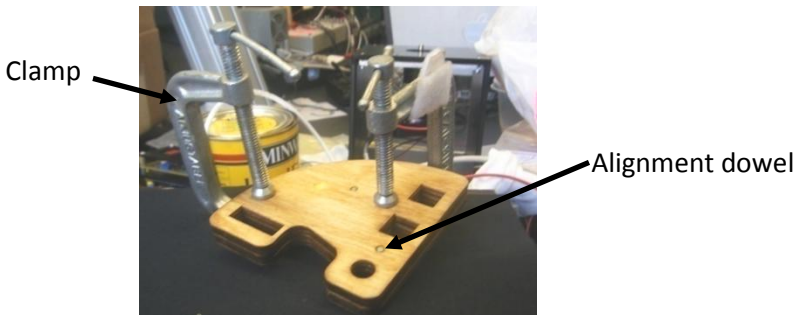

Figure 30: Part clamping procedure

VIII.2. Initial Assembly

The frame of the structure was assembled using the puzzle piece slots to align the two sides of the frame to the base in the correct positions. They were then glued in place, clamped, and left to dry. The frame can be seen in Fig. 31. Next, the shaft was fit into the sides of the frame and the motor was mounted to the left wall of the frame using M3 screws.

Figure 31: Frame assembly

VIII.3. Rotating Components

Figure 32, p.27, shows the final rotating assembly. The following sections detail the construction of this mechanism.

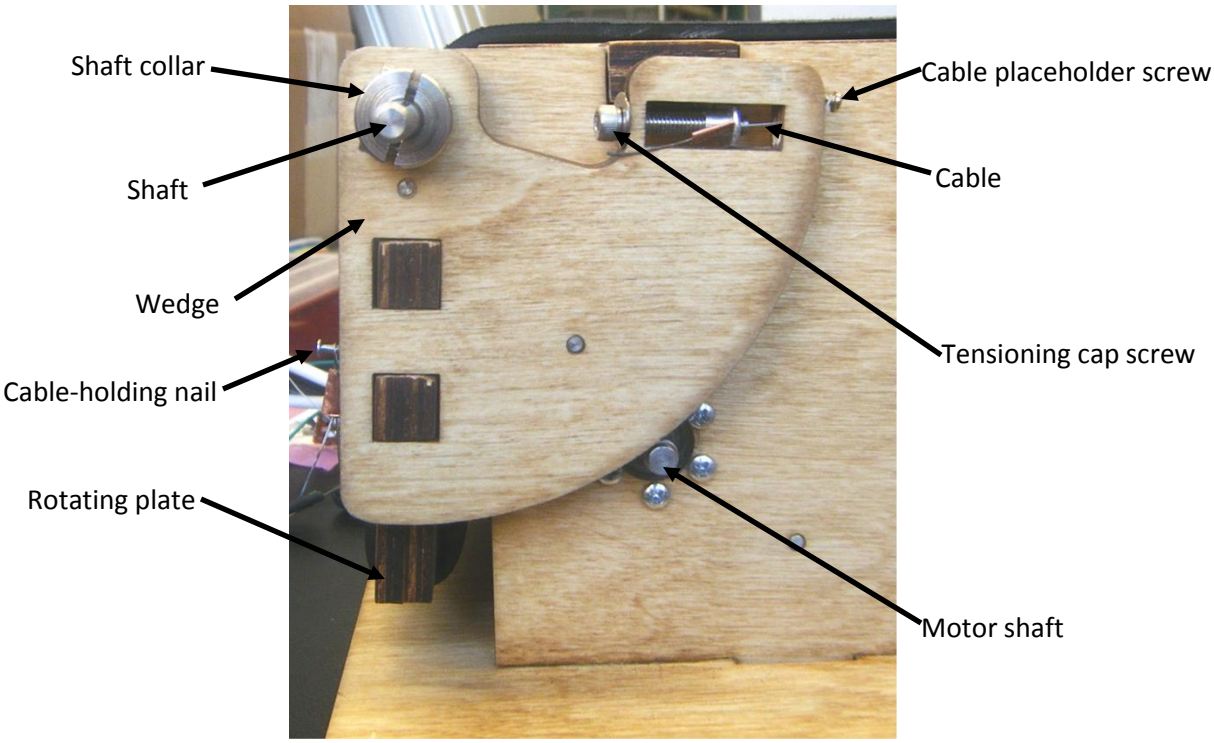

Figure 32: Capstan drive rotating assembly

VIII.3.1. Preparation and preliminary assembly

First, a hole to be used for subsequent cable tensioning was drilled into the capstan drive wedge, as seen in Fig. 33. The hole was hand drilled using a 5/32" size drill bit. Next, two flanged bearings were press fit into both sides of the two wedges. One-quarter inch inner diameter washers were placed on both ends of the shaft, followed by the two wedges, with the rotating plate put in position between them using the puzzle piece slots. Shaft collars were place on the ends of each shaft to ensure that all parts stay in place and that the bearings were properly preloaded. The bearing-washer-shaft collar assembly can be seen in Fig. 34.

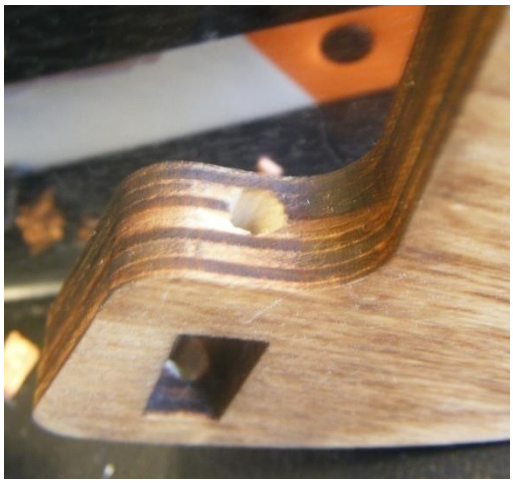

Figure 33: Through hole on wedge for cable tensioning

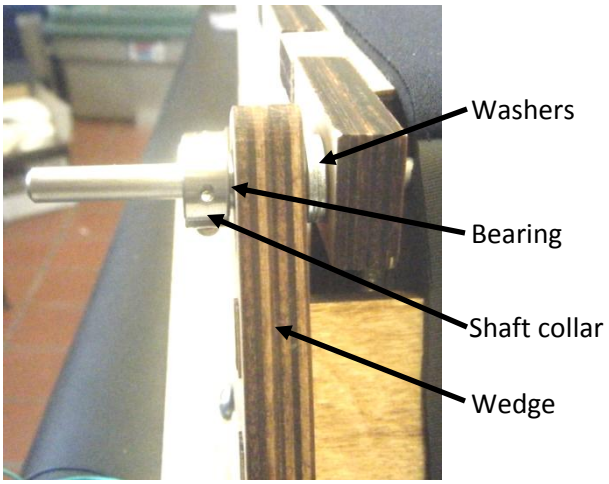

Figure 34: Bearing pre-load assembly

Additionally, a mechanical stop mechanism was added using two screws, as seen in Fig. 35. The first screw was permanently attached to the wedge, and the second screw was placed in the frame wall. The purpose of the mechanical stop assembly was to inhibit the wedge from rotating past the desired angle, as seen in Fig. 36. This mechanism was added to the wedge on the opposite side of the motor.

Figure 35: Mechanical stop in disengaged position

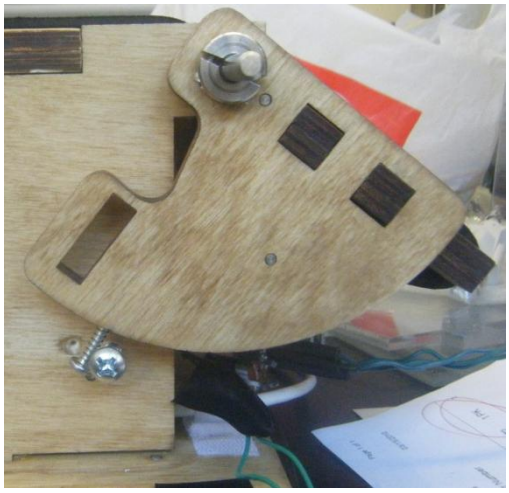

Figure 36: Mechanical stop mechanism in engaged position

VIII.3.2. Cable tensioning

Once all parts were in place, the cable was attached. For tensioning the cable, a No. 8 threaded insert was grinded to fit inside of the slot on the wedge and a hole of 1/32" diameter was drilled into the flange to allow the cable to go through. The cable was put through this hole and permanently positioned by crimping a small piece of copper tubing over the cable, as seen in Fig. 37. The cable was then fed through the hole on the wedge and a No. 8 cap screw was used to position the threaded insert, also seen in Fig. 37.

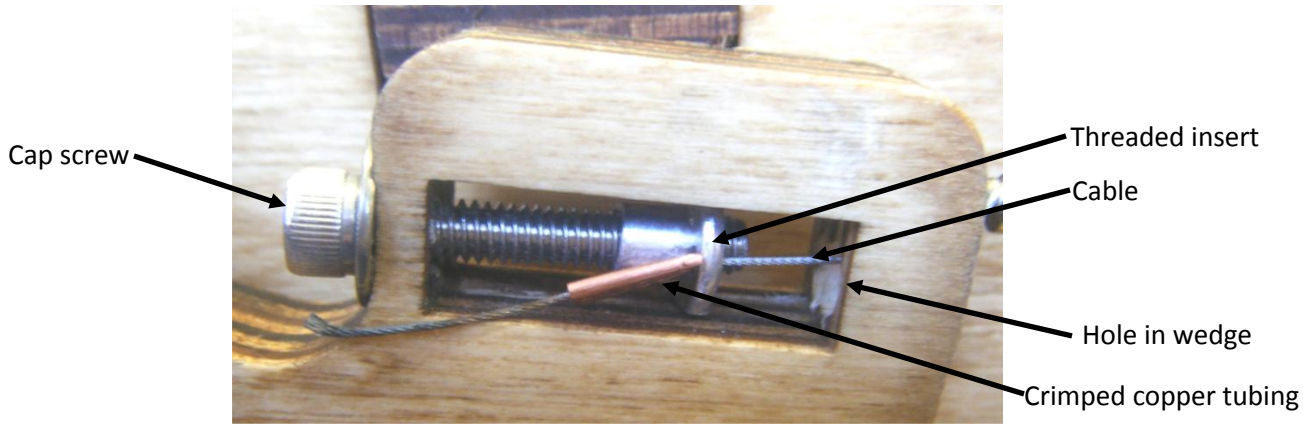

Figure 37: Cable tensioning mechanism

The cable was positioned on the wedge using a screw place holder, as seen in Fig. 38, p.29, and was then wrapped around the motor shaft three times (Fig. 39, p.29). A loop was created on the other end using the copper tube to crimp to the cable. This loop was then put over the head of a nail placed on the opposite side of the wedge (Fig. 40, p.29), while ensuring that the cable stayed on the outer radius of

the wedge. The cable was then tensioned properly by tightening the cap screw/threaded insert assembly.

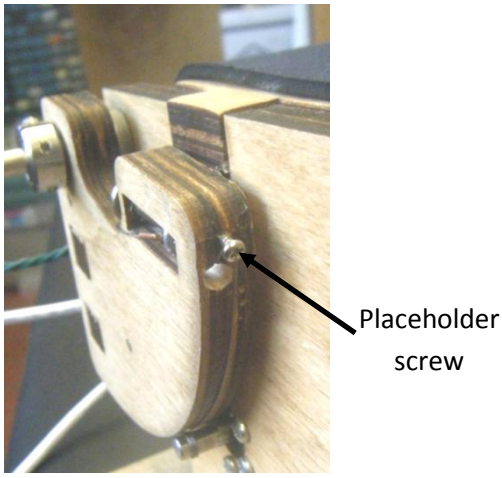

Figure 38: Cable positioning screw

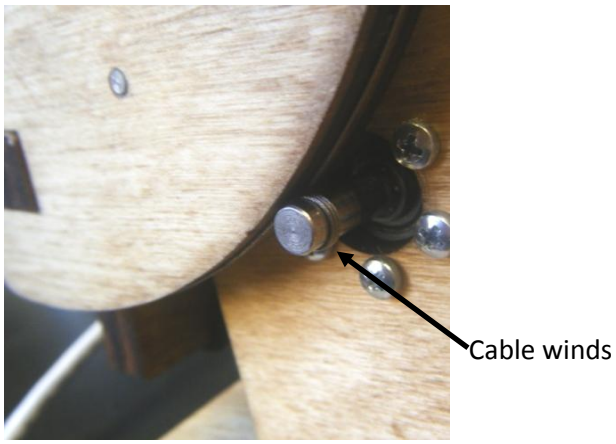

Figure 39: Motor cable winds

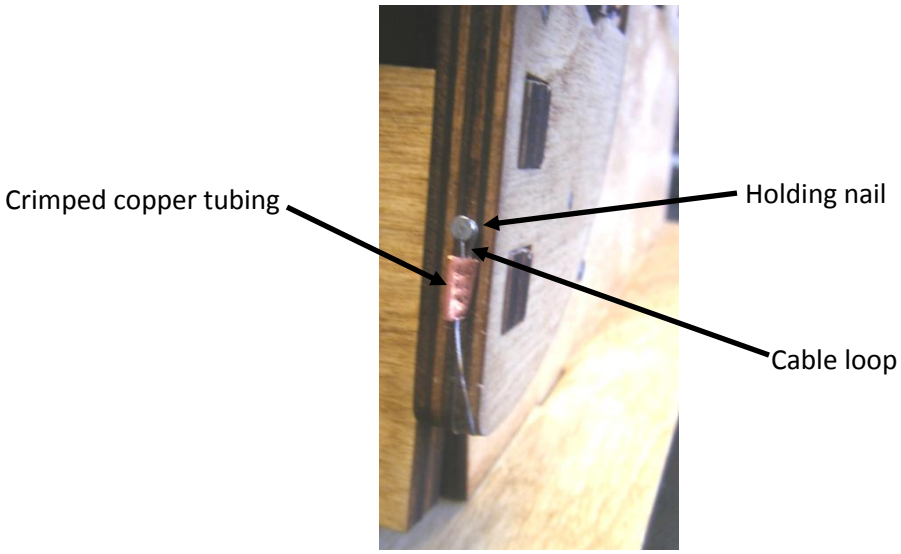

Figure 40: Permanently attached cable holder

VIII.4. Electrical Assembly

In order to program the motor, the electrical circuitry, shown in block diagram form in Fig. 41, was created and placed inside of the device. A computer controlled an Arduino MEGA microprocessor through a USB cable. This microprocessor was used to send signals to an Advanced Motion Controls Model No. R04 48046-0143 amplifier through an RC filter and voltage divider. The RC filter was used to block certain frequencies and allowing others to pass through. The voltage divider was used to split the voltage in half to allow half of the voltage range to turn the motor clockwise and the other half to turn the motor counter-clockwise. The amplifier was powered by a Power-One power supply, and then two inductors were connected in series with the Maxon RE40 motor. The inductors were added to eliminate a loud buzzing noise created by the motor. The position of the motor was then read by a U.S. Digital encoder and sent back to the microprocessor. The microprocessor then changed the signal it sent to the

amplifier based on the encoder readings. Additionally, all components were connected to a common ground to ensure that the current will flow through the circuit in the desired direction. Once all of the components were connected, the microprocessor was ready to be programmed. Specific electrical connections, including resistors, capacitors, and inductors, are shown in Fig. 42.

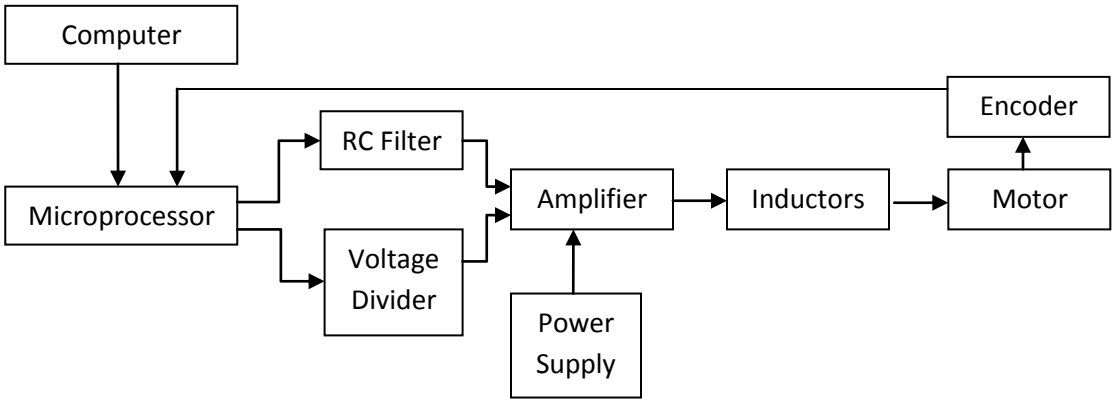

Figure 41: Schematic of electrical circuitry used to operate motor

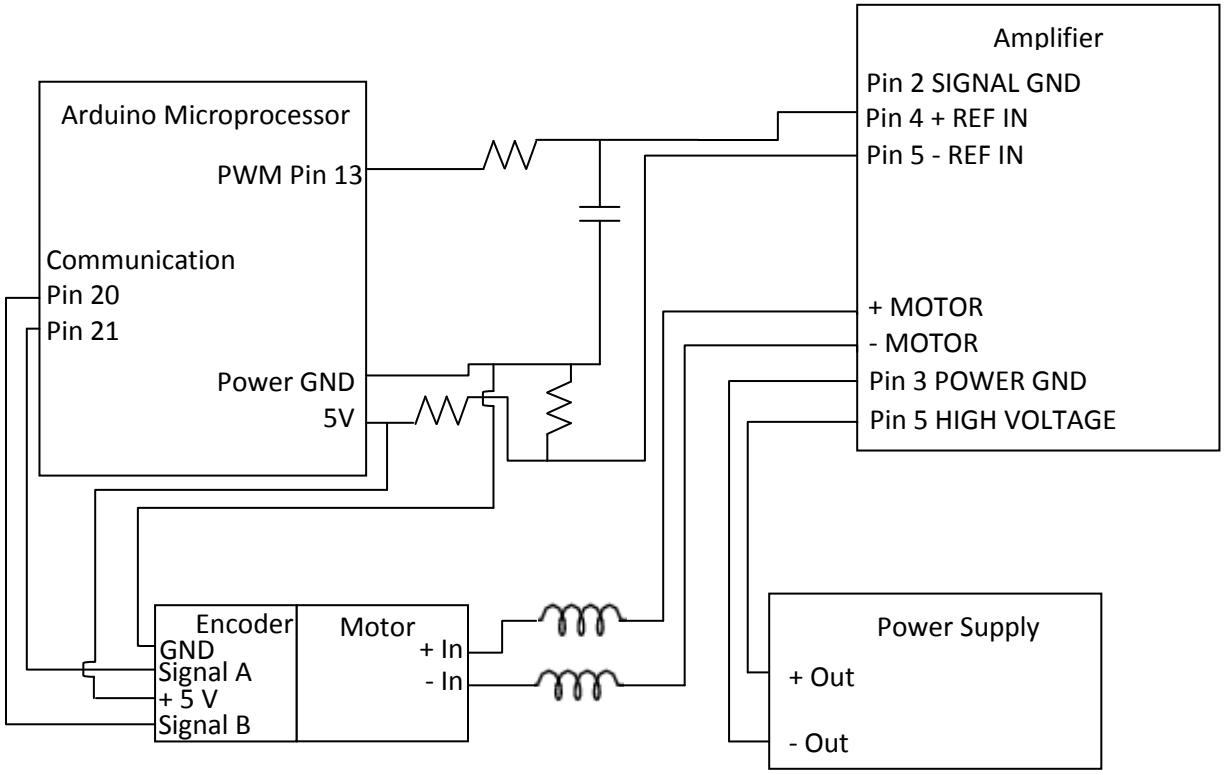

Figure 42: Detailed schematic of all electrical connections

VIII.5. Final Assembly

After all electrical work was complete, the top and back of the frame were put in place using the puzzle piece slots. Neoprene fabric was then aligned across the top of the box and stretched underneath the

rotating plate. It was secured with Velcro® adhesive fasteners and re-enforced stitching. This completed the assembly of the device.

IX. VALIDATION RESULTS

Using C++ code on the Arduino microprocessor, which can be found on Appendix D, the range of motor speeds was determined for both clockwise and counter clockwise directions. The range was determined by inputting various voltages and visually inspecting the motor's rotation. The voltage at which the motor stopped running was determined to be 0.25 V. Voltages above 0.25 V turned the motor counterclockwise, while voltages below 0.25 V turned the motor clockwise.

A potentiometer was then integrated into the circuitry to allow motion to be controlled by the potentiometer knob's position. The variable resistance provided by the potentiometer correlated to varying voltages sent to the motor. This allowed control of the angle of the rotating plate. However, the motion produced by torque control was unreliable since it did not guarantee the angles reached during the rotation, because only the output speed of the motor was controlled.

To gain better control of the angle of the rotating plate, the Arduino code was altered to include position control instead of torque control. Using the encoder on the motor shaft, the Arduino made it possible to specify positions of the rotating plate. The potentiometer was used as a substitute for the analog input provided by the BCI 2000 software. When the knob was turned right, the plate extended; likewise, when the knob was turned left, the plate contracted. By using position control, we were able to create a fully controlled device that was able to be integrated into the current UM-DBI project setup.

X. DISCUSSION

The subsequent sections will detail how the device meets the engineering specifications, and provide suggestions on how to change the device to better meet these specifications.

X.1. Analysis of Engineering Specifications

Table 7 below provides a summary of the engineering specifications, the target values for these specifications, and whether these values have been achieved by the device.

Table 7: Ability of final design to meet engineering specifications

Engineering Specifications	Target Value	Met value (y/n)
Response time	≤ 0.125 s	Y
Noise level	≤ 5 dB or constant	Y
Size settings	≥ 3	Y
Number of moving components	≤ 2	Y
Feedback settings	3	Y
Dimensions	20" x 20"	Y
Weight	≤ 25 lb	N
Setup time	< 15 minutes	Y

X.1.1. Response time

The target value for response time was less than 0.125 seconds. The device met this specification with a response time of 50 ms. Using the Arduino code, delays can be changed to vary the response time. The measured response time was based on turning the knob of a potentiometer, and when the device is actually implemented In the UM-DBI project setup we believe the response time will improve due to fact that only electrical signals will be transferred to and from the device instead of the physical input provided by the potentiometer.

X.1.2. Noise level

The target value for noise level was less than 5 dB or constant. We met the specification using both torque control and position control. However, when first using torque control, the motor produced a noticeable buzzing noise, which was eliminated by adding an inductor to the electrical circuitry. When in position control, the motor only runs when the knob is turned, and runs at low torques that do not produce a noticeable noise.

X.1.3. Size settings

The target value for size settings was 3 sizes. The device met this value since it was designed with the average person's hand size in mind. While demonstrating our device at the Design Expo, we observed a variety of hand sizes and all of them were able to use the device appropriately. However, we felt that the implementation of a strap over the user's fingers would guarantee that all users will feel the same motion. Adding a strap could limit the number the sizes of hands and proper consideration of strap size as well as comfort will need to be taken into account.

X.1.4. Number of moving components

The target value for number of moving components was less than or equal to 2. Our device met this value, and the only moving component is the rotating plate. The device was designed to press fit the shaft into the frame, and shaft collars were placed on the ends to ensure it did not move.

X.1.5. Feedback settings

The target value for feedback settings was at least 3. Our device met this specification, and can have an unlimited number of feedback settings depending on the Arduino code. In the code, the signal inputs can be divided into any number of intervals to correlate with motor voltages in torque control. With position control, the range of angles can be changed depending on the input signals, changing the speed that the motor needs to turn to achieve that position.

X.1.6. Dimensions

The target value for dimensions was less than 20" x 20". Our device meets this specification, and is 12" by 13.5" which will easily fit on the table in the UM-DBI project setup. Additionally, the device could fit on a standard laptop table, allowing portability of the device.

X.1.7. Weight

The target value for the weight of the device was less than 25 lbs. Our device is currently heavier than this, and weighs approximately 35 lbs. Most of this weight comes from the electrical components, specifically the power supply and inductor, which are currently packaged inside of the structure. It is possible to move these components outside of the structure by replacing the wires with longer ones, allowing the components to rest on the surface outside of the device. This would reduce the weight of the device, and additionally allow for ease of access to all components in case the electrical circuitry needs to change.

X.1.8. Setup time

The target value for the setup time of the device was less than 15 minutes. Our device meets this specification, and only requires an electrical outlet to function. Additionally, the Arduino microprocessor currently must be plugged into a computer to generate power, but it could be rewired to receive power directly from the power supply on the device.

X.2. Additional Critiques

In addition to the previous engineering specifications, the device can be made visually absent. This feature was discussed in preliminary meetings with our sponsors. Currently we fulfill this by using an external wooden structure that is placed over the device once the user's hand is positioned. While this is effective in preventing the user from seeing the motion, the device could be redesigned to include a built-in casing attached to the base to block the user's line of sight.

While the device is currently coated with neoprene to provide comfort and cleanliness, the flat position of the hand required to feel the motion could be changed to be more natural to the user. This could be done by adding a mass of material where the palm of the user's hand will be placed to simulate the natural curved position of a hand in its relaxed position.

XI. RECOMMENDATIONS

In order to improve the device, we recommend the changes shown in the subsequent sections.

XI.1. Hand Positioning

To feel more natural to the user, we recommend changing the location of the hand on the device. This could be done by lowering the top plate to allow the user's fingers to rotate about an axis that is more natural. It is also possible to have the top plate be on an angle to better align the axis of rotation with the knuckles on a hand.

XI.2. Wedge Sizing

We chose the wedge angle to be 40° when designing the wedge's arc length. To increase the range of motion of the rotating plate, we recommend increasing the arc length of the wedge. This will allow for greater flexibility when controlling the position of the rotating plate.

XI.3. Wedge Clearance

When tensioning the cable, it was difficult to fit an Allen wrench comfortably in the cut-out area of the wedge. There currently is not enough clearance, and we recommend making this cut out area big enough to fit the required Allen wrench.

XI.4. Electrical Circuitry

The electrical circuitry currently inside of the device is not completely secured. We used a plastic circuit board, which prevented us from soldering the connections permanently. We recommend replacing this plastic circuit board with a board that can be soldered.

XII. FUTURE WORK

In order to move forward with the haptic feedback device, the following steps must be taken:

- Create BCI technology interface
- Modify existing IRB to include haptic feedback provisions
- Install haptic feedback device in the UM-DBI project laboratory
- Conduct clinical study based on IRB at UM-DBI project location to test the effect of haptic feedback on BCI learning rates

XIII. CONCLUSION

In an effort to increase the learning rate for BCIs, Dr. Jane Huggins proposed the use of haptic feedback in addition to the visual feedback that is currently provided at the UM-DBI project setup. The project goal is to design a device that will provide haptic feedback without disrupting the testing environment. By using a motion common to daily activity, such a finger raising, it is believed that it is possible to provide the user a sense of agency of the motion so that the imagined motion required to generate EEG signals can correlate with physical feedback. The device created met the majority of engineering specifications, such as fast response time, size settings, audibly absent, and quick setup time. The one engineering specification that the device did not meet was that it be portable and weigh less than 25 lbs; however, the electrical components currently packaged inside the device can be moved external to the device to fulfill this specification. Once properly interfaced with the BCI software, the device will provide a user with 40° of motion to correspond with the imagined movement. Through the creation and implementation of this device, it is hoped that haptic feedback will be proven to increase BCI learning rate.

XIV. ACKNOWLEDGEMENTS

We would like to thank Professor Brent Gillespie, Dr. Jane Huggins, John Baker, Phil Bonkoski, Bob Coury, Marv Cressey, and Carmela Lee for their help with our project throughout the semester. Without their help, we would not have been able to complete this project.

XV. REFERENCES

[1] Febo Cincotti, Laura Kauhanen, Fabio Aloise, et al., "Vibrotactile Feedback for Brain-Computer Interface Operation," Computational Intelligence and Neuroscience, vol. 2007, Article ID 048937, 12 pages, 2007. doi: 10.1144/2007/48937

[2] T. Hinterberger, N. Neumann, M. Pham, et al., "A multimodal brain-based feedback and communication system," *Experimental Brain Research*, vol. 154, no. 4, pp. 521–526, 2004.

[3] M. Pham, T. Hinterberger, N. Neumann, et al., "An auditory brain-computer interface based on the self-regulation of
slow cortical potentials," *Neurorehabilitation and Neural Repair*, vol. 19, no. 3, pp. 206–218, 2005.

[4] F. Nijboer, A. Furdea, I. Gunst, et al., "An auditory brain computer interface (BCI)," to appear in *Journal of Neuroscience
Methods*.

[5] D. J. McFarland, L. M. McCane, and J. R. Wolpaw, "EEG based communication and control: short-term role of feedback,"
IEEE Transactions on Rehabilitation Engineering, vol. 6, no. 1, pp. 7–11, 1998.

[6] C. Neuper, A. Schlogl, and G. Pfurtscheller, "Enhancement of left-right sensorimotor EEG differences during feedback regulated motor imagery," *Journal of Clinical Neurophysiology*, vol. 16, no. 4, pp. 373–382, 1999.

[7] Ramos, A., Halder, S., Birbaumer, N., "Proprioceptive Feedback in BCI," 2009 4th International IEEE/EMBS Conference on Neural Engineering, NER '09 2009

[8] McFarland DJ, Miner LA, Vaughan TM, et al. Mu and beta rhythm topographies during motor imagery and actual movements. *Brain Topogr*. Spring 2000;12(3):177-86.

[9] von Holst E, Mittelstaedt H. "The Principle of reafferance: Interactions between the central nervous system and the peripheral organs" (translated by P.C. Dodwell and reprinted from Die Naturwissenschaften (1950)). In: Dodwell PC, editor. Perceptual Processing: Stimulus equivalence and pattern recognition. Appleton-Century-Crofts; New York: 1971. pp. 41–71.

[10] Feinberg, Irwin. "Efference copy and corollary discharge: Implications for thinking and its disorders," Schizophr Bull, vol. 4, no. 4, pp. 636-640, 1978.

[11] J. Vidal, "Toward Direct Brain–Computer Communication", in Annual Review of Biophysics and Bioengineering, L.J. Mullins, Ed., Annual Reviews, Inc., Palo Alto, Vol. 2, 1973, pp. 157-180.

[12] Maxon Precision Motors, Inc. "Maxon DC motor: RE 40," Fall River: 2006.

[13] Granta Design Limited. 2009. *CES Selector Version 5.1.0*. Cambridge.

[14] Ashby, Michael. Material Selection in Mechanical Design. 3rd ed. Maryland Heights: Elsevier Science & Technology Books, 2005. 66-85. Print.

APPENDIX A: QFD FORMATION

Once the customer requirements were determined and translated into engineering metrics, the QFD was created. In order to determine the requirement's importance, each requirement was compared to the others and rated with a 0 or 1, depending on which requirement held more importance to the final design. The requirements were then ranked depending on the total score from the evaluation process. This comparison can be found in Table A1 below.

Table A1: Comparison of customer requirements to determine weight

	Simple	Perceptually Absent	Size	Corresponding Feedback	Portable	Safe for User	Initial Adjustability for Comfort	Varying Feedback Levels	Believability	Total Score	Weight
Simple	--	1	1	0	1	0	0	0	1	4	4
Perceptually Absent	0	--	1	0	1	0	1	1	0	4	4
Size	0	0	--	0	1	0	0	0	0	1	2
Corresponding Feedback	1	1	1	--	1	0	1	1	1	7	8
Portable	0	0	0	0	--	0	0	0	0	0	1
Safe for User	1	1	1	1	1	--	1	1	1	8	9
Initial Adjustability for Comfort	1	o	1	0	1	0	--	1	0	4	4
Varying Feedback Levels	1	0	1	0	1	0	0	--	0	3	3
Believability	0	1	1	0	1	0	1	1	--	5	7

Using the weights determined above, the QFD was then created, as seen in Figure A1, p. 10. Table A2 provides a key in determining the correlation rankings found in the main body of the QFD.

Table A2: QFD legend

QFD Ranking	Connection Between Customer Requirement and Engineering Metric
9	Strongly related
3	Somewhat related
1	Weakly related
(blank)	Not related

	Engineering Metrics	Number of Moving Components	Noise	Hand Mount Height above Table	Width	Length	Response Time	Set-Up Time	Weight	Size Settings	Feedback Settings
Customer Requirements	**Wt**										
Simple	4	9						3			
Audibly Absent	4		9								
Size	2			9	9	9			3		
Corresponding Feedback	8						9				
Portable	1			3	3	3		3	9		
Safe for User	9						1				1
Initial Adjustability for Comfort	4									9	
Varying Feedback Levels	3						3				9
Believability	7										
Weighted Total		36	36	21	21	21	81	15	15	36	36
Importance Ranking		6	6	3	3	3	10	1	1	6	6
Target Values		≤ 2	< 5 dB or constant	≤ 2"	≤ 20"	≤ 20"	≤ 1/8 second	< 15 minutes	<25 lbs	≥ 3	≥ 2

Figure A1: QFD

The QFD was helpful in determining the engineering metrics that are of the utmost importance in the design process in order to fulfill customer requirements. Using the QFD, the following engineering metrics were determined to be the focus of the design:

- Response time
- Number of moving components
- Noise level
- Size setting
- Feedback settings

APPENDIX B: EXPERIMENTAL TESTING

The results of the experimental testing of the top three selected concept designs were organized based on the subject's choice of most believable motion and the time it took each subject to believe the motion was believable. Table B1 below shows the amount of time it took each subject to believe the motion as well as the average time it took for users to believe the motion. If the subject was unable to believe the motion then it was reported as "n/a".

Table B1: Amount of time for subjects to believe motion

Subject	Finger Raising	Moving Material	Wrist Rotation	Vote
1	45	n/a	n/a	1
2	n/a	60	n/a	2
3	45	n/a	n/a	1
4	60	45	n/a	2
5	35	75	75	1
6	75	70	n/a	2
7	45	n/a	n/a	1
8	35	60	n/a	1
9	n/a	n/a	n/a	n/a
10	n/a	65	n/a	2
11	45	55	75	1
12	60	75	n/a	1
13	45	n/a	n/a	1
14	30	60	n/a	1
15	60	n/a	n/a	1
16	60	n/a	n/a	1
17	45	60	n/a	1
18	35	n/a	n/a	1
19	60	45	70	2
20	45	n/a	n/a	1
Average	48.53	60.91	73.33	
Total that felt motion was believable	17	11	3	

Table B2 below shows the distribution of votes for each design based on age and sex.

Table B2: Distribution of votes for believability based on age and sex

	Total Votes	Age 20 Votes	Age 21 Votes	Age 22 Votes	Age 23 Votes	Female Votes	Male Votes
Finger Raising	14	1	3	7	1	10	4
Moving Material	5	0	2	1	2	3	2
Wrist Rotation	0	0	0	0	0	0	0
Undecided	1	0	0	1	0	0	1
Total	20	1	5	9	3	13	7

APPENDIX C: FINAL DESIGN

C.1. Assembly Drawings

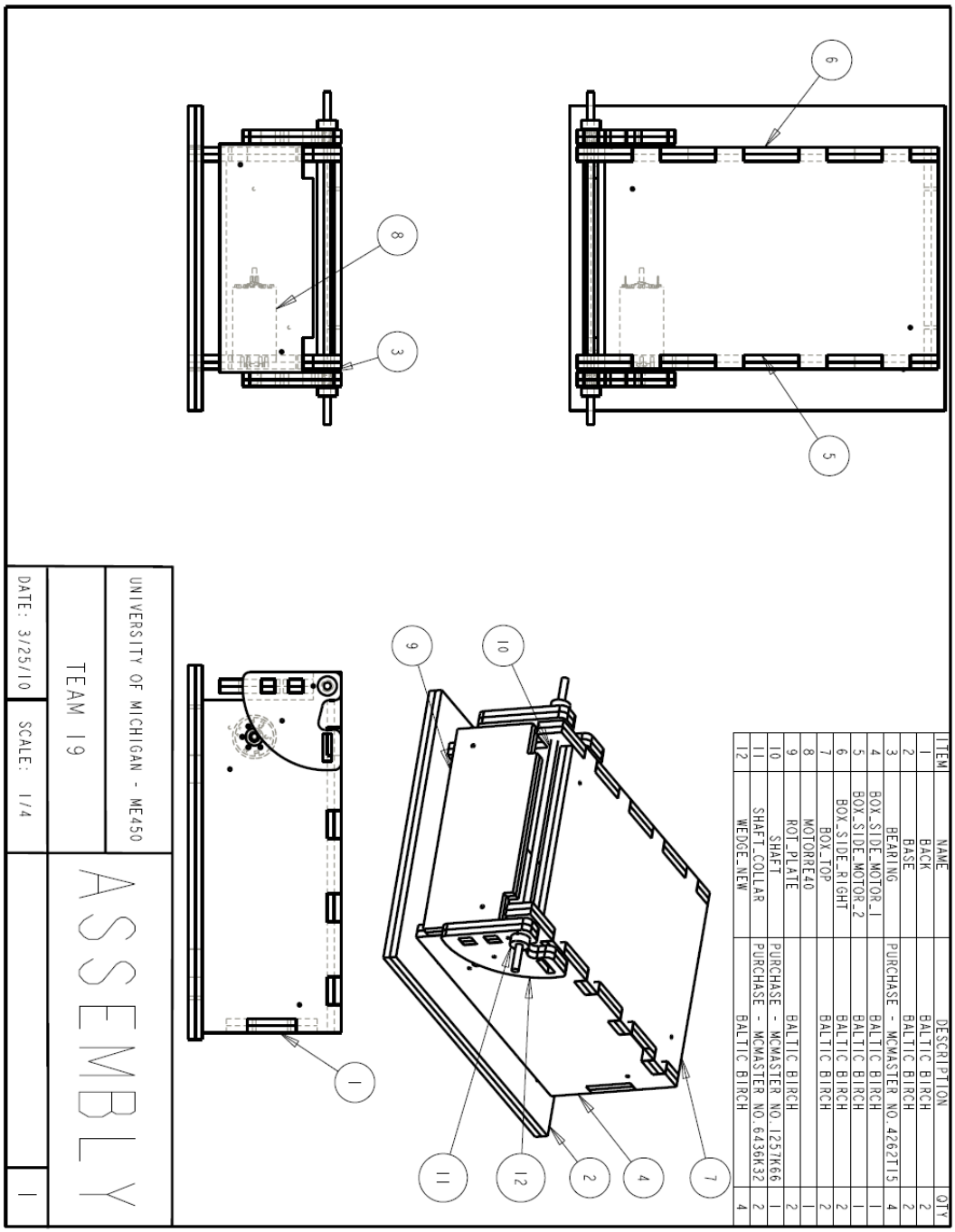

Figure C1: Full assembly

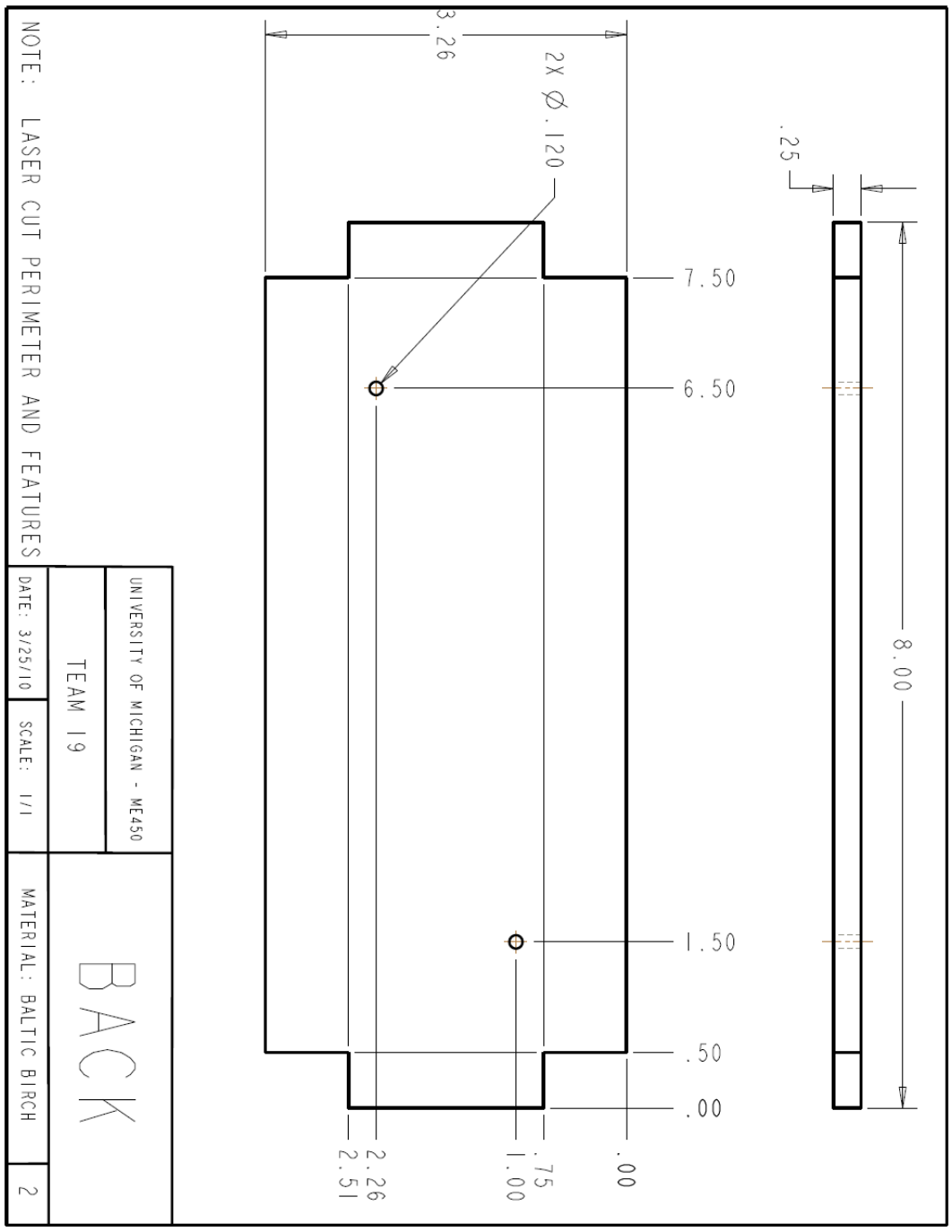

Figure C2: Back

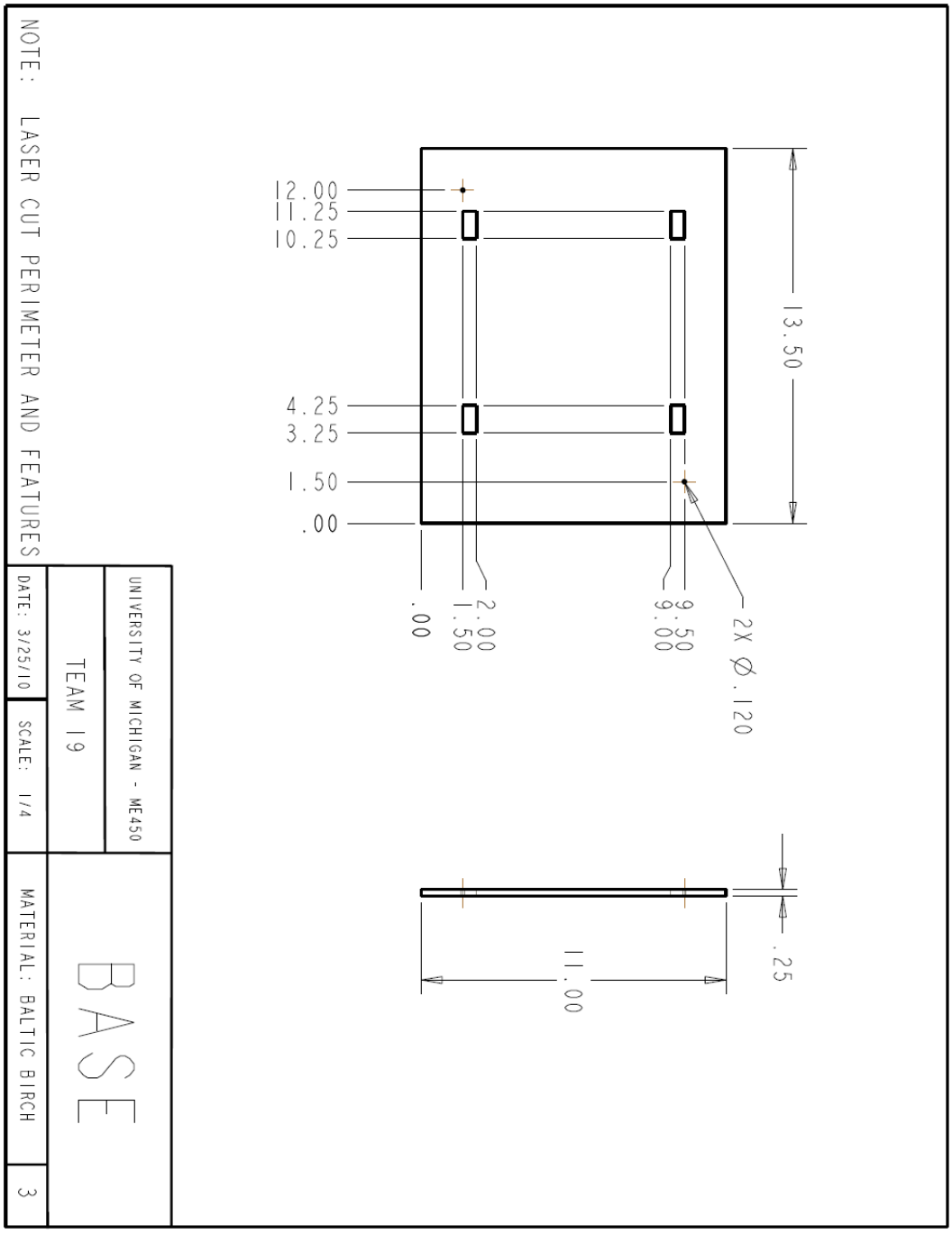

Figure C3: Base

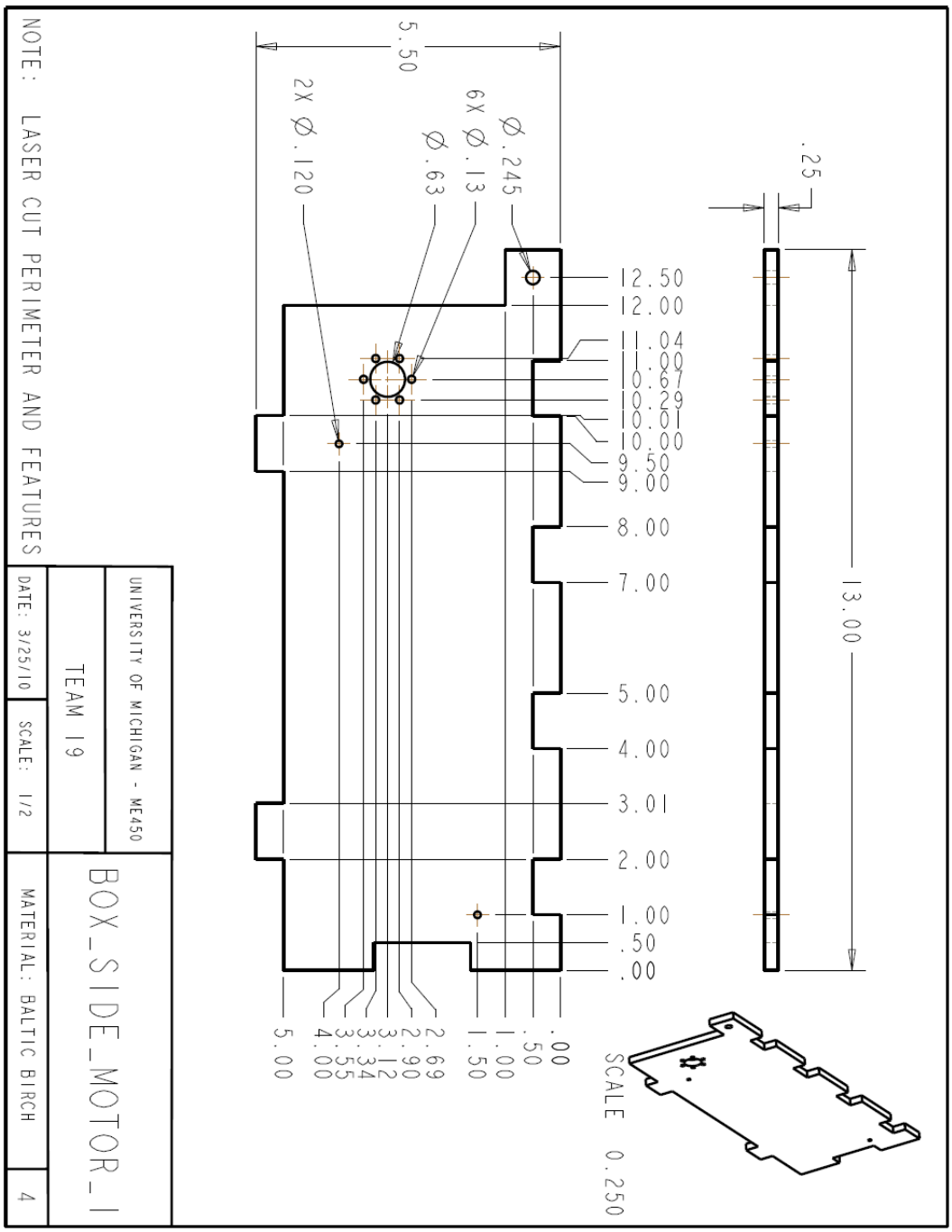

Figure C4: Box side motor 1

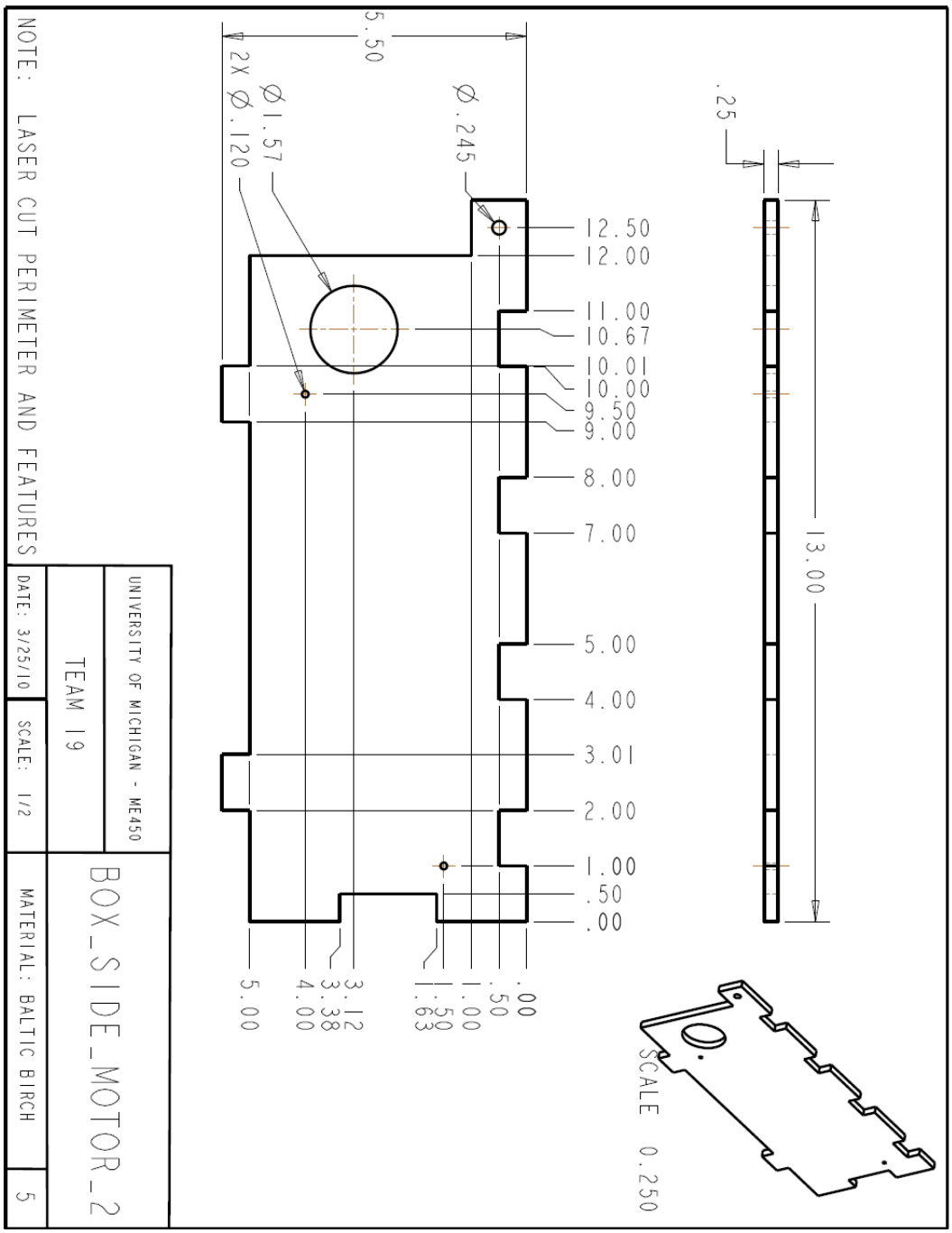

Figure C5: Box side motor 2

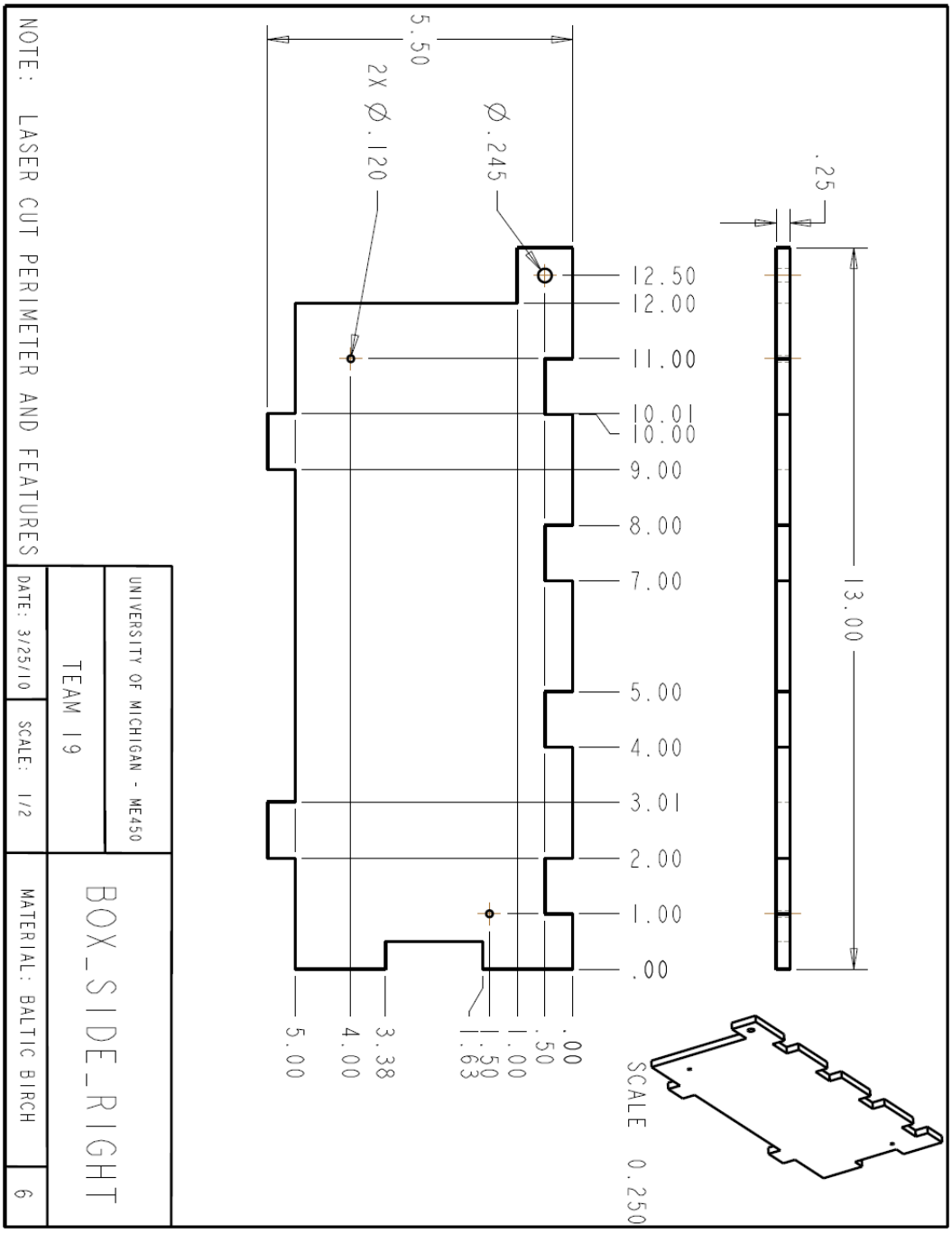

Figure C6: Box side right

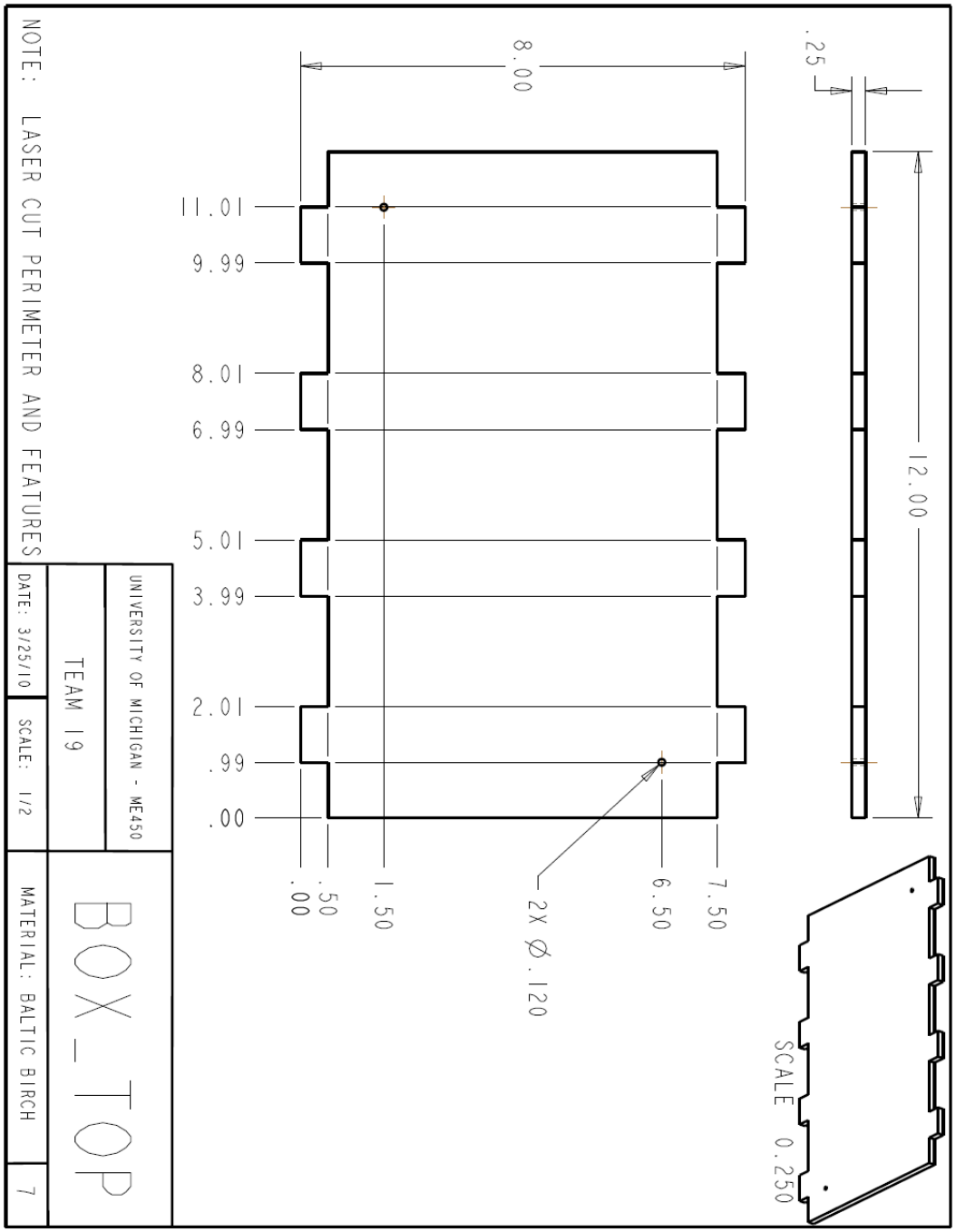

Figure C7: Box top

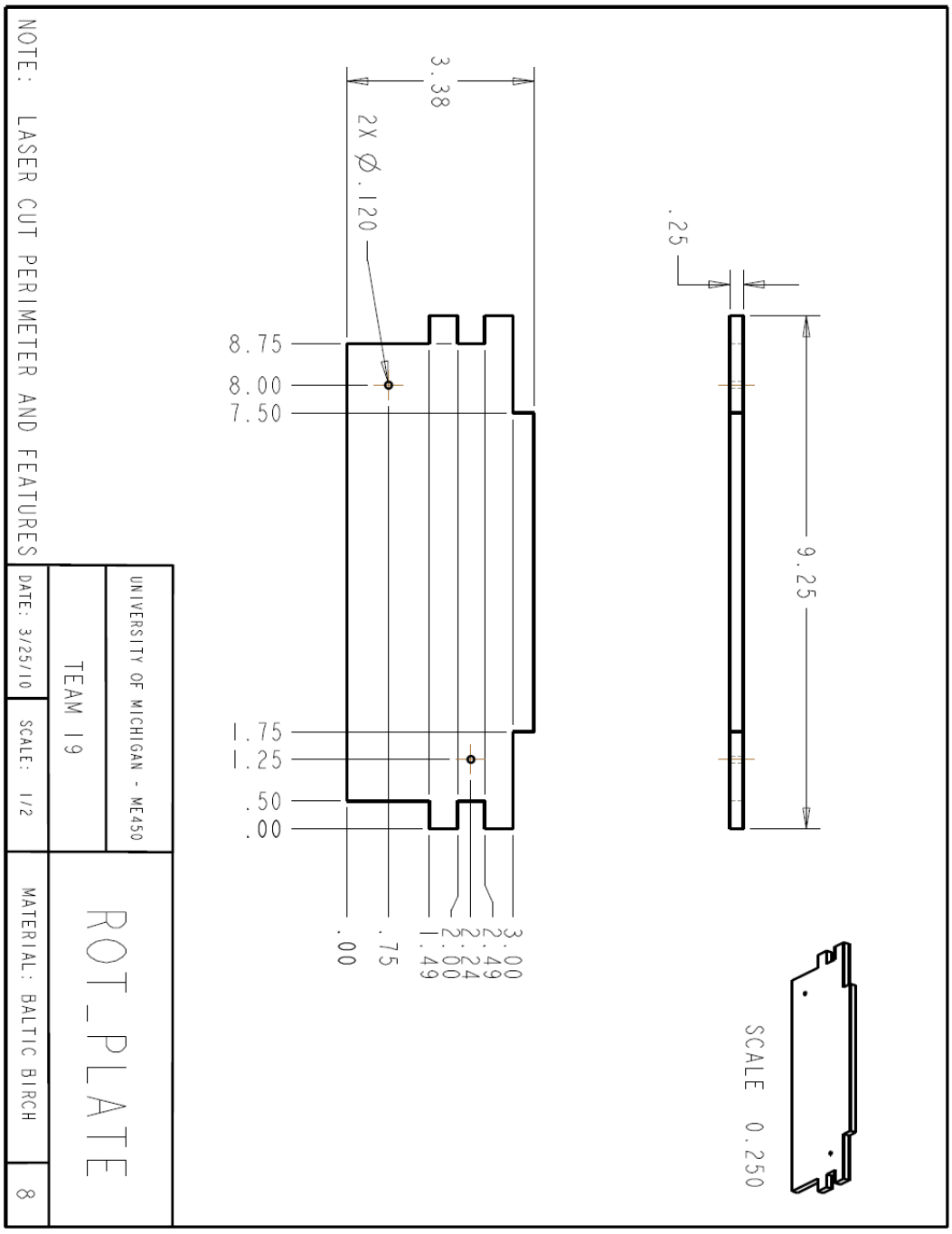

Figure C8: Rotating plate

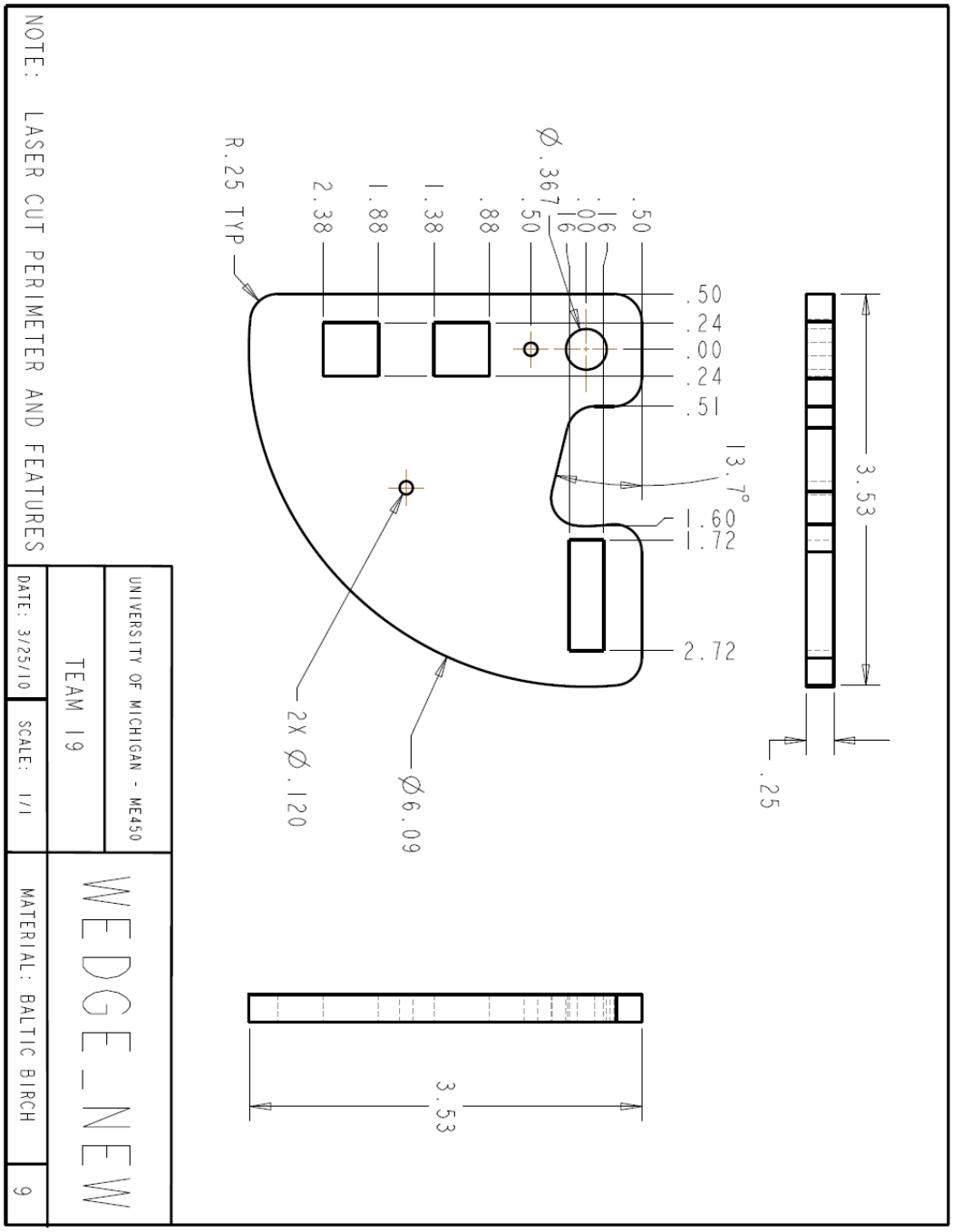

Figure C9: Wedge

C.2. Complete BOM

Table C1 below contains the ordering information for all of the purchased components used directly in the execution of the final design.

Table C1: Purchased components

Item	Quantity	Source	Catalog Number	Unit Cost	Contact	Notes
1/4" drive shaft	1	McMaster-Carr	1257K66	$6.62	Mcmaster.com	--
Two-piece shaft collar	2	McMaster-Carr	6436K32	$6.03	Mcmaster.com	--
Cable	--	Sava Cable	2018	$0.447/ft	Sava Cable – Thomas Lawrence	Used in wedge actuation
Double shielded ball bearing for ¼" shaft	2	McMaster-Carr	4262T15	$13.51	Mcmaster.com	--
Stainless steel 1/8" dowel pins	1 pack	McMaster-Carr	90145A481	$13.11/pack of 100	Mcmaster.com	For component assembly

A list of all components manufactured on-site in the University of Michigan undergraduate machining shop can be found in Table C2.

Table C2: Manufactured components

Component	Material	Fabrication Process
Motor side 1	Baltic birch	Laser cut
Motor side 2	Baltic birch	Laser cut
Motor stand base	Baltic birch	Laser cut
Frame side	Baltic birch	Laser cut
Capstan drive wedge	Baltic birch	Laser cut
Rotating plate	Baltic birch	Laser cut
Frame top	Baltic birch	Laser cut
Back	Baltic birch	Laser cut

C.3. CES for Neoprene

The following is the CES for Neoprene from [13].

Polychloroprene (CR, unreinforced)

No warranty is given for the accuracy of this data. Values marked * are estimates.

General properties

Designation

Polychloroprene / Polychlorobutadiene / Chloroprene rubber (CR)

Density 0.0444 - 0.047 lb/in^3

Price * 2.33 - 2.56 USD/lb

Tradenames

Neoprene, Baypren, Denka Chloroprene, Butaclor, Skyprene

Composition overview

Composition (summary)

Poly-chloroprene (mainly trans isomer), chemical formula: (CH2-CCl=CH-CH2)n. 40% Cl. Typically cured by metal oxides (MgO & ZnO at ~5phr).

Base Polymer
Polymer class Elastomer
Polymer type CR
% filler 0 %
Filler type Unfilled

Composition detail

Polymer 100 %

Mechanical properties

Young's modulus 2.39e-4 - 3.05e-4 10^6 psi
Compressive modulus * 2.39e-4 - 3.05e-4 10^6 psi
Flexural modulus * 2.39e-4 - 3.05e-4 10^6 psi
Shear modulus 7.98e-6 - 0.00102 10^6 psi
Bulk modulus * 0.218 - 0.29 10^6 psi
Poisson's ratio 0.48 - 0.495
Shape factor 1.5
Yield strength (elastic limit) 1.74 - 3.48 ksi
Tensile strength 1.74 - 3.48 ksi
Compressive strength * 2.09 - 4.18 ksi
Flexural strength (modulus of rupture) * 3.4 - 5.99 ksi
Elongation 750 - 950 %
Elongation at yield 750 - 950 %
Hardness - Shore A 40 - 46
Fatigue strength at 10^7 cycles * 0.696 - 1.39 ksi
Fracture toughness * 0.754 - 0.791 ksi.in^1/2
Mechanical loss coefficient (tan delta) 0.06 - 0.17
Compression set at 23°C 2 - 10 %
Compression set at 70°C 7 - 17 %
Compression set at 100°C 15 - 25 %
Tear strength 16.7 - 20.9 ft.lbf/in^2

Impact properties

Impact strength, notched 23 °C 90.4 - 95.2 ft.lbf/in^2
Impact strength, notched -30 °C 90.4 - 95.2 ft.lbf/in^2

Thermal properties

Glass temperature -54.4 - -36.4 °F
Maximum service temperature 216 - 234 °F
Minimum service temperature -67 - -40 °F
Thermal conductivity 0.0867 - 0.116 BTU.ft/h.ft^2.F
Specific heat capacity 0.502 - 0.525 BTU/lb.F
Thermal expansion coefficient 112 - 136 µstrain/°F

Electrical properties

Electrical resistivity 1e17 - 1e19 µohm.cm
Dielectric constant (relative permittivity) 6.5 - 8.1
Dissipation factor (dielectric loss tangent) 0.03 - 0.04
Dielectric strength (dielectric breakdown) 386 - 599 V/mil

Optical properties
Refractive index 1.55 - 1.57
Transparency Translucent

Absorption, permeability
Water absorption @ 24 hrs * 0.6 - 0.8 %
Permeability (O2) 21.6 - 67.6 cm³.mm/(m².day.atm)

Durability: flammability
Flammability Self-extinguishing

Durability: fluids and sunlight
Water (fresh) Excellent
Water (salt) Excellent
Weak acids Acceptable
Strong acids Limited use
Weak alkalis Excellent
Strong alkalis Excellent
Organic solvents Limited use
Oils and fuels Limited use
UV radiation (sunlight) Fair
Oxidation at 500C Unacceptable

Primary material production: energy, CO2 and water
Embodied energy, primary production 1.04e4 - 1.15e4 kcal/lb
CO2 footprint, primary production 3.49 - 3.86 lb/lb
Water usage 3.49e3 - 1.05e4 in^3/lb

Material processing: energy
Polymer molding energy * 853 - 941 kcal/lb

Material processing: CO2 footprint
Polymer molding CO2 * 0.63 - 0.695 lb/lb

Material recycling: energy, CO2 and recycle fraction
Recycle
Recycle fraction in current supply 1.34 - 1.48 %
Downcycle
Combust for energy recovery
Heat of combustion (net) * 1.83e3 - 1.92e3 kcal/lb
Combustion CO2 * 1.39 - 1.46 lb/lb
Landfill
Biodegrade
A renewable resource?

Notes
Typical uses
Wire & cable coating, hose, automotive timing belts, wet suit sponge, soles and heels, rubber coating for fabrics, roof coatings. Also, adhesives -- pre-eminent among elastomeric adhesives due to combination of polarity and strength.
Other notes
Like NR, CR is capable of strain-induced crystallization resulting in superior mechanical properties. Strengths: Mechanical properties and fatigue resistance second only to natural rubber (NR). Superior to NR in

its chemical, oil, and heat resistance, and lower gas permeability. Good ozone resistance compared to other diene-based 'R' rubbers. Good metal bonding. Fire resistance.
Limitations: Less resistant to low temperature stiffening than NR (compounding can improve this). Poorer set and creep than NR. Relatively high water adsorption.

Reference sources

Data compiled from multiple sources. See links to the References table. Range of mechanical properties from Vanderbilt Rubber handbook.

Links

ProcessUniverse
Producers
Reference
Shape

APPENDIX D: MICROPROCESSOR PROGRAMMING

D.1. Torque Control

The following code was sent to the Arduino microprocessor to control the motor using torque values.

```
const int readPin=1;
const int writePin=13;

void setup() {

   Serial.begin(9600);
   pinMode(writePin, OUTPUT);

}

void loop() {
   int cmd;
   float temp;
   int gain=0;
   int offset=65;
   //temp = 0-5.

   temp=analogRead(readPin);
   //Serial.println(temp);
   temp=temp*5.0/1024.0;
   //Serial.println(temp);

   if(temp>=0&&temp<2) cmd=55;
   if(temp>=2&&temp<3) cmd=63;
   if(temp>=3&&temp<=5) cmd=72;
   Serial.println(cmd);
   //cmd = gain*temp + offset;

   analogWrite(writePin,cmd);

}
```

D.2. Position Control

The following code was sent to the Arduino microproccesor to control the motor using position values.

```
/* This will be code used in Demo tmrw.
Same as demoProgram except encodercode is added
*/

#define ENCPINA 21
#define ENCPINB 20

const int readPin=1;
```

```
const int writePin=13;

int led = 13;

   int cmd;
   float q_actual;
   float q_desired;
   float cmd_degrees;
   float Gain=3.0;

volatile int encPos = 0;

void setup() {

  pinMode(writePin, OUTPUT);

    //Begin encoder stuff

  analogWrite(led,0);

  pinMode(ENCPINA, INPUT);
  pinMode(ENCPINB, INPUT);

  digitalWrite(ENCPINA,HIGH);
  digitalWrite(ENCPINB,HIGH);

  attachInterrupt(2, readEncoderA, CHANGE);
  attachInterrupt(3, readEncoderB, CHANGE);

  Serial.begin(19200);

}

void loop() {

   q_desired = analogRead(readPin)*30.0/1024.0;

   q_actual=encPos/278.3; // 278.3=11 pulses/deg * 25.3 (mechanical adv).

   cmd_degrees = Gain*(q_desired - q_actual);

   cmd = 63 + cmd_degrees * 255.0/360.0;
   analogWrite(writePin,cmd);

/*
  Serial.print("enc: ");
  Serial.print(encPos);
  Serial.print(",  q_actual: ");
```

```
  Serial.print(q_actual);
  Serial.print(",  q_desired: ");
  Serial.print(q_desired);
  Serial.print(", cmd_degrees: ");
  Serial.print(cmd_degrees);
  Serial.print(", cmd: ");
  Serial.print(cmd);
  Serial.print("\n");
  */
}

//Encoder functions:
void readEncoderA(){
  if(digitalRead(ENCPINA) ^ digitalRead(ENCPINB))
    encPos++;
  else
    encPos--;
}

void readEncoderB(){
  if(digitalRead(ENCPINA) ^ digitalRead(ENCPINB))
    encPos--;
  else
    encPos++;
}
```

APPENDIX E: INITIAL PROJECT PLAN

Preliminary project planning included the formation of a working timeline and consideration of the project budget challenges.

E.1. Timeline

In order to ensure timely project completion, the milestones that needed to be reached were first established. Using these milestones, the design planning stages and prototyping phases were then determined. A timeline for project completion can be found in Table E1 below.

Table E1: Project timeline

Task	Duration
Preliminary Sponsor Meeting	Jan 21
Design Review #1	Jan 26
Initial Design Phase	Jan 27 – Feb 4
Prototyping Phase #1	Feb 5 – Feb 17
Design Review #2	Feb 18
Redesign	Feb 19 – Feb 26
Prototyping Phase #2	Feb 27 – Mar 17
Design Review #3	Mar 18
Safety Evaluation	Mar 19 – Mar 20
Final Design Changes	Mar 21 – Mar 23
Manufacturing of Final Design	Mar 24 – Mar 31
Design Review #4	Apr 1
Deliver Project to Sponsor	Apr 2
Subject Testing	Apr 3 – Apr 9
Design Expo	Apr 15

The ultimate project goal is to present the working final design to the Rehabilitation Engineering lab on April 2. This allows for one week of subject testing using the BCI along with haptic feedback. By following this timeline, preliminary information regarding the effect of haptic feedback on the BCI learning process will be presented at the Design Expo.

E.2. Budget Considerations

In the preliminary design phases, the biggest consideration in the $400 budget was determined to be the required operational noise level. Because the function of the system cannot be audibly perceivable, a great deal of the budget will be spent on either minimizing the noise level or creating constant noise in order to mask the operational sounds.

APPENDIX F: DESIGN ANALYSIS ASSIGNMENT

F.1. Material Selection for Functional Performance

While our device features a stainless steel shaft and stainless steel cable used in the capstan drive, the most prevalent materials are the wood used for the main components of the device and the fabric used for the covering of the device.

F.1.1. Baltic birch

The structure of the device has been fabricated using Baltic birch since it was readily available in the lab, inexpensive, and provided adequate support. The subsequent subsections explore other possible materials for use in the structure and validate our final decision to use birch.

F.1.1.1. Material requirements

The function of Baltic birch is to maintain support and structure for the device. The wood serves as both an enclosure of the electrical components as well a support for the hand resting on the top of the device. The objective is to maximize the strength of the material while simultaneously maintain a low material weight since a key engineering specification is that the device be portable. Another objective is to minimize the cost of the material. Constraints on the material used for this function come from the durability of the material since the rotating plate is moving a component. Additionally, the melting point of the material is of concern, because it is possible the enclosed power supply and inductor could heat up after prolonged use.

F.1.1.2. Material indices

The material indices were determined to be similar to that of a light, stiff beam as noted in Ashby's Materials [14] and represented using Eq. F1 below where E is the Young's modulus and ρ is the density of the material.

$$M_1 = \frac{E^{1/2}}{\rho} \quad \text{(Eq. F1)}$$

While the cross-sectional area is dictated by the design of the device, the objective in this case would still be to minimize its mass while maintaining a strong structure. It is also possible to apply additional material indices, such as the one shown in Eq. F2 below if we want to look at cases where only the Young's modulus, or stiffness of the material, can be altered.

$$M_2 = E \quad \text{(Eq. F2)}$$

F.1.1.3. Possible candidates

Table F1, p.58, lists five material choices as well as their density, price, Young's modulus, yield strength, and maximum service temperature. All five of these properties are relevant to choosing a material that is light, inexpensive, strong, durable, and resistant to high temperatures.

Table F1: Material candidates for device structure

Material	Density (lb/ft^3)	Price (USD/lb)	Young's modulus (10^6 Psi)	Yield strength (ksi)	Maximum service temperature (°F)
Birch	0.022-0.028	0.32-0.64	1.99-2.44	7.35-8.98	248-284
Plywood	43.7-49.9	0.15-0.422	1-1.89	1.31-4.35	212-266
Acrylic	72.4-76.2	1.17-1.29	0.325-0.551	7.8-10.5	107-134
Aluminum	237-248	8.28-12.4	49.7-56.6	50.8-85.3	3.64E3-3.8E3
Concrete	144-162	0.019-0.028	2.18-3.63	0.145-0.435	1.7E3-2.24E3

F.1.1.4. Final material selection

Based on the calculations of the material indices for each material listed in Table F1 above, we believe Baltic bitch is the best material choice for the structure of the device for a number of reasons. 1.) The density of Baltic birch is at least two magnitudes less than that of any of the other structure options. 2.) It has a reasonable price for the amount needed for the device. 3.) The material has a great enough Young's modulus to support the structure and the user's hand. 4.) Baltic birch has a Yield strength more than adequate for the setup. 5.)It can resist possible temperatures reached by the electrical circuitry. While plywood has very similar properties to birch, the density is much greater, and since the objective aims to decrease the weight of the device, birch would still be the best choice for the main component material.

F.1.2. Neoprene

The top of the device has been covered with neoprene fabric. The subsequent subsections explore other possible materials for use in covering the device as well as validate our final decision to use neoprene.

F.1.2.1. Material requirements

The function of the material used to cover the top of the device is to provide comfort for the user as well as maintain a hygienic testing environment. This material has no other function for the device nor does it provide any structural support. The objective of the material is to minimize cost so that the material can be easily replaced and maximize comfort, which is a subjective measure. Constraints on the material stem from its durability and flexibility (it must be able to cover the rotating plate without buckling). It is also important that the material be relatively lightweight so as not to contribute a disproportional amount of mass compared to that of the structure.

F.1.2.2. Material indices

To calculate the material indices, we used Eq. F1 and Eq. F2 as shown on p.57.

F.1.2.3. Possible candidates

Table F2, p.59 lists five material choices for covering the top of the device as well as their density, price, percent elongation, and moldability. The percent elongation and moldability are important to determine how easy the material can be integrated with the device, since the material must be stretched to prevent buckling during rotation.

Table F2: Material candidates for device covering

Material	Density (lb/ft^3)	Price (USD/lb)	Elongation (%)	Moldability
Neoprene	76.8-78	2.33-2.56	100-800	4.0-5.0
Foam (polyurethane)	2.37-4.37	1.32-1.41	10-175	1.0-4.0
Flexible foam	4.37-7.18	1.41-1.5	9-115	1.0-4.0
Butyl rubber	56.2-57.4	1.69-1.86	400-500	4.0-5.0
Polyisoprene rubber	58.1-58.7	1.32-1.45	500-550	4.0-5.0

F.1.2.4. Final material selection

While both types of foam maintain low densities and are thus, lightweight materials, they have low values for percent elongation and also have unfavorably low moldability ranking. Neoprene is the best material for its ability to elongate up to 800%, however, its high density and expensive cost make rubber a more viable option. However, neoprene does offer resistance to water and oils, so one could argue that it is worth the money.

F.2. Material Selection for Environmental Performance

The total volume of each of the materials required was determined based on the engineering drawings. Based on the analysis of the functional performance for the structure material, it was evident that the material would be some type of wood; thus, for the analysis, we compared birch with yellow pine using SimaPro. An illustration of the emissions determined using SimaPro and translated into Excel can be found in Fig. F1.

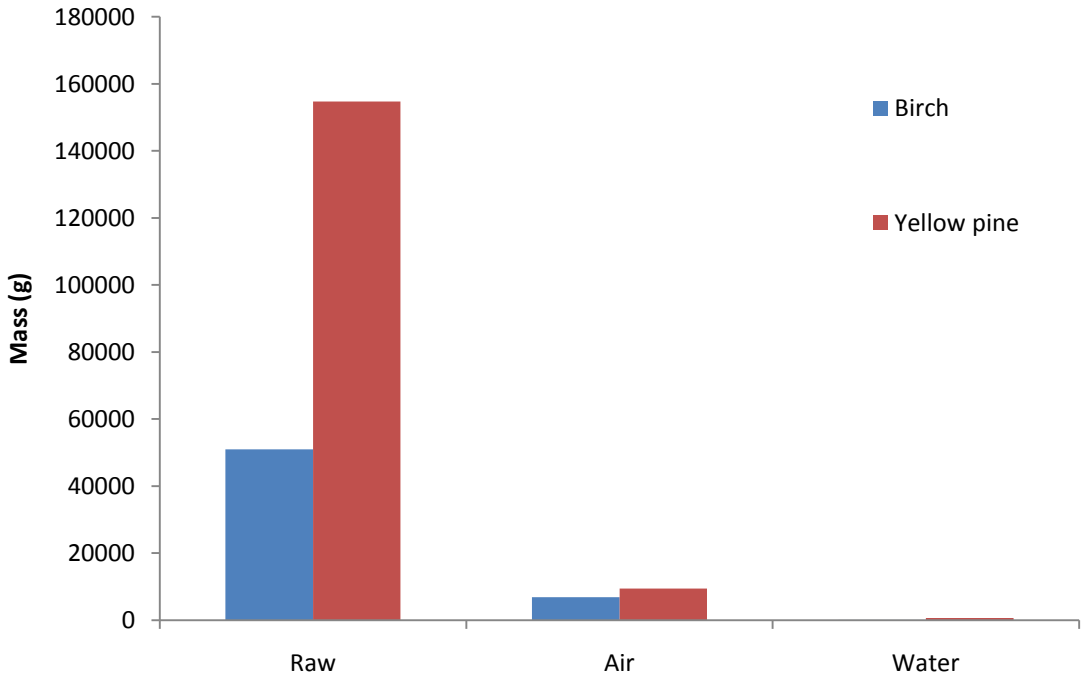

Figure F1: Comparison of emissions for types of wood

Yellow pine ranks higher in percentage points in every measure of damage assessment, thus, birch is a clear choice of material for optimizing environmental performance.

In order to analyze material for the device covering it was necessary to choose comparable materials, since neoprene is not available in the SimaPro database. We chose high impact polystyrene (HIPS) since it is frequently used in packaging material and could be appropriate as a cover for our device. We chose to compare it with polybutadiene, a synthetic rubber commonly used in tires, since it is a material resilient to fluid and can be manufactured with rubber to increase its flexibility. An illustration of emission caused by the use of these materials can be found in Fig. F2.

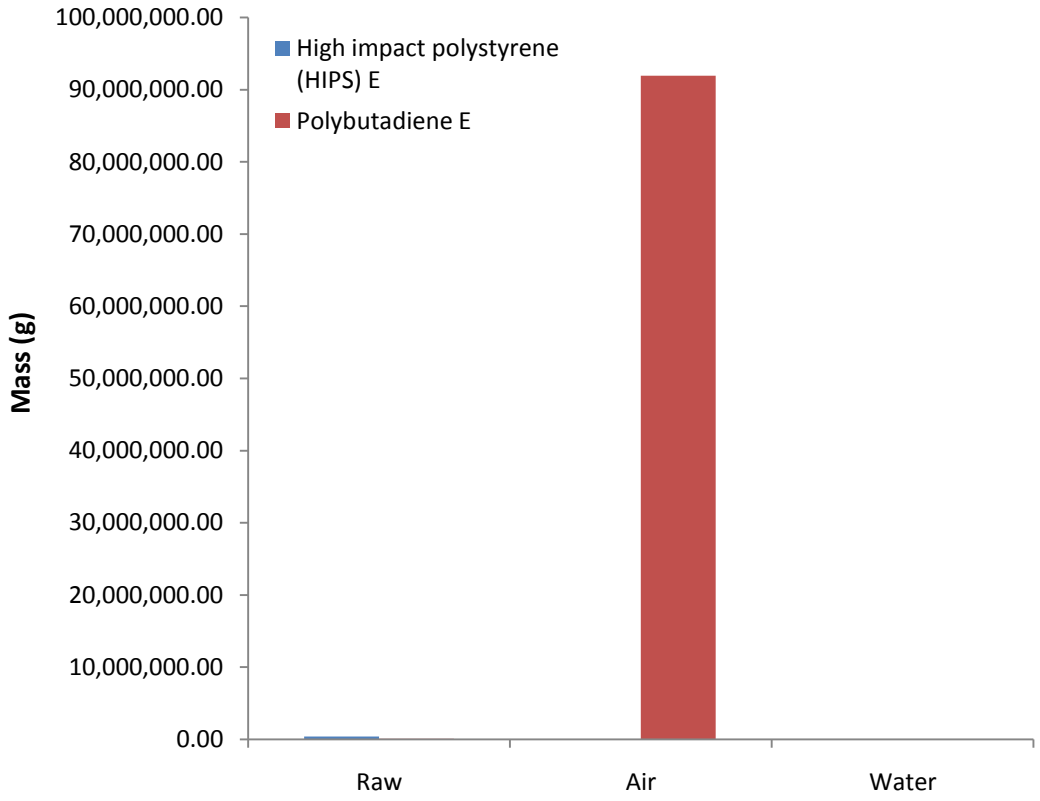

Figure F2: Comparison of emissions for types of padding material

While HIPS has high percentages of carcinogens, high effect on the ozone layer and ecotoxicity, polybutadiene has equally high percentages on climate change, resp. organics, and resp. inorganics. Thus when both materials are observed having a single score, polybutadiene has a greater sum of emissions, leading us to prefer HIPS for its environmental performance.

F.3. Manufacturing Process Selection

The following sections detail the determination of the manufacturing process including the production volume and the materials to be used.

F.3.1. Production volume

In order to determine the potential production volume, some assumptions must be made. The ultimate goal of the device is to test the hypothesis that haptic feedback will reduce the time it takes a user to achieve a high degree of accuracy using BCI technology. If this hypothesis can be proven, then the

device could have many uses across the globe. For our purposes, we will concentrate on the focus of Dr. Huggins' UM-DBI project, which is concentrated on helping mainly ALS patients use BCI technology to interact with the world around them. Based partially on the number of ALS patients in advance stages of the disease around the world, we have determined the production volume to be approximately 10,000 units.

F.3.2. Material one: baltic birch

All of the main components of the prototype were manufactured out of Baltic birch. At the determined production volume of 10,000, the most efficient way to manufacture these components is to use a process called nibbling where the desired profile is created by successive "bites" from a small punch. This process is ideal because it provides a better finish for larger parts such as the frame components. Additionally, the smaller, more complex parts will be more easily and cleanly made using this process. Also, the tolerances this process is capable of and the finish are within the requirements for the device [13].

Economically, our batch size is slightly small to warrant the necessary investment in equipment. However, these machines can be used to create nearly any part, so they can be used in other processes when the production volume for our device is reached. The tooling costs are not high, and the labor intensity required to complete the nibbling process is very low. Therefore, the cost for employees to facilitate the creation of the birch components is low [13].

Additionally, the surface of the birch components would need to be coated. We are choosing to perform a texturing process, because it is cost effective while still providing an aesthetically pleasing appearance. The equipment and tooling costs are kept relatively low without sacrificing wear resistance or looks [13].

F.3.3. Material two: neoprene

The covering of the device was made out of neoprene. At the production volume of 10,000, the material would be purchased in bulk from an outside supplier such as Thermoplastics Rubber Systems, Inc. The material would then be cut to size using a stamping process, which is cost effective given the production volume we are considering [13].